Development of an Array of 3-D Position Sensitive Virtual Frisch-grid Detectors

Aleksey Bolotnikov

Department of Nonproliferation and National Security

INSTRUMENTATION DIVISION SEMINAR
February 6, 2013

Introduction: Current status and trends in CZT detector development

Expectations:

- Room-temperature operation
- Large effective area (similar to NaI)
- High-energy resolution (similar to HPGe)
- High 3D position resolution (imaging devices)

Reality that shapes a current state of technology:

- Material non-uniformity (twins, Te inclusions, and subgrain boundaries)
- Low availability and high cost of detector grade material
- Small volume of crystals, < 6 cm^3

Strong demand, broad area of applications:

- Medical
- Industrial
- Security
- Basic science

Temptation

Specific features of CZT detectors

- CZT is used for making X- and gamma-ray detectors
- CZT is different from Si and HPGe:
  - Slow semiconductor (holes are ~20 time slower than electrons)
  - High-resistivity material => no depletion layer but negative space charge is built up
  - CZT crystals have low surface resistivity in comparison to bulk (surface is like a conductive skin that affects electric field distribution inside detectors)
  - Single-type carrier device => suffer from the induction effect (i.e., amplitude dependence on interaction points locations)
  - <u>Non-uniform material due a high content of defects</u>

Defects in CZT crystals

- Two types of extended defects in today's CZT material that limit performance of detectors (point defects can be corrected):
  - Te inclusions
  - Subgrain boundaries
- Both types of defects exist in commercial CZT materials regardless of growth techniques or vendors
- Vendors cannot specify contents of the subgrain boundaries in their crystals because they mainly use IR microscopy to screen defects in CZT material which cannot reveal subgrain boundaries directly
- Most effective techniques are:
  - White beam X-ray diffraction topography
  - Chemical etching of crystal surfaces, e.g. Nakagawa solution

Diffraction topographs helps to select good crystals

In reflection mode, one can see defects exiting the surface of the crystals

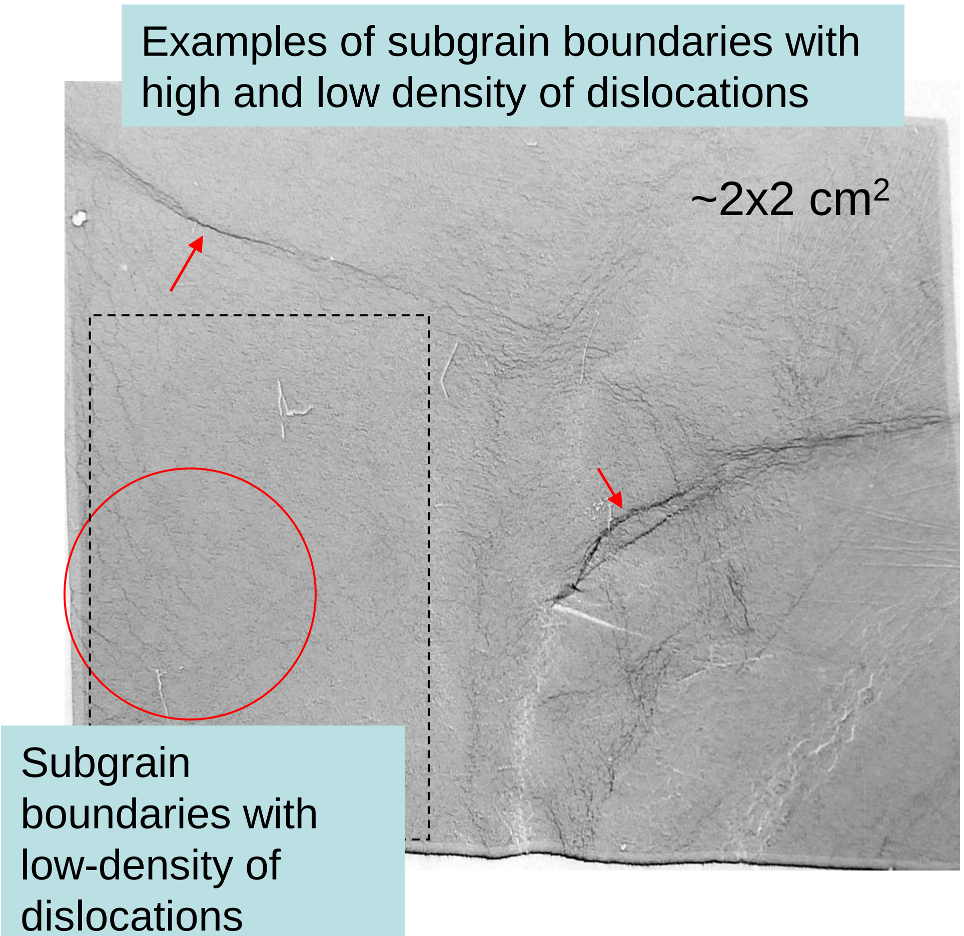

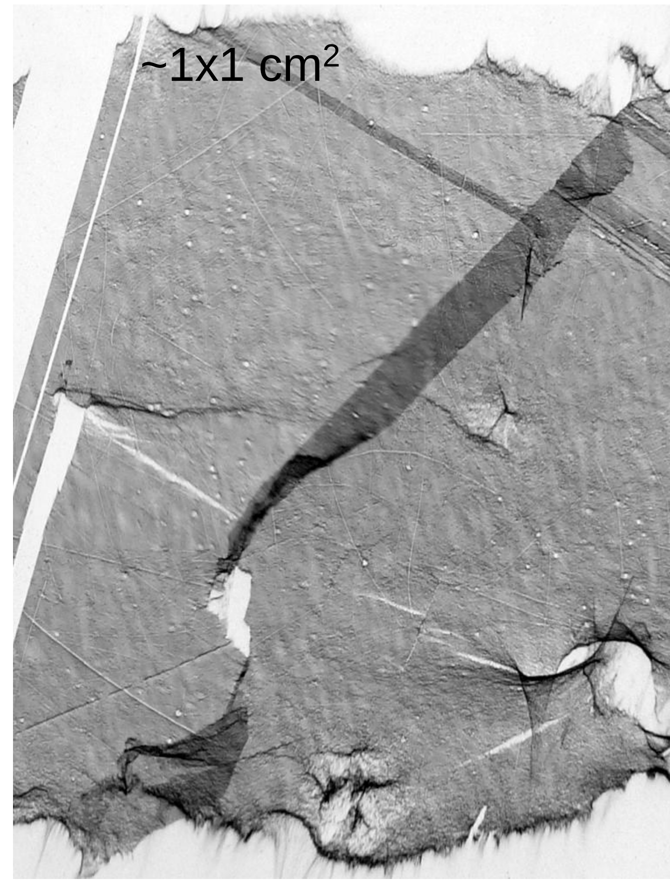

3D reconstructed IR images of Te inclusions

Randomly distributed Te inclusions and decorated dislocations and subgrain boundaries

1.1x1.4x6 mm^3 regions

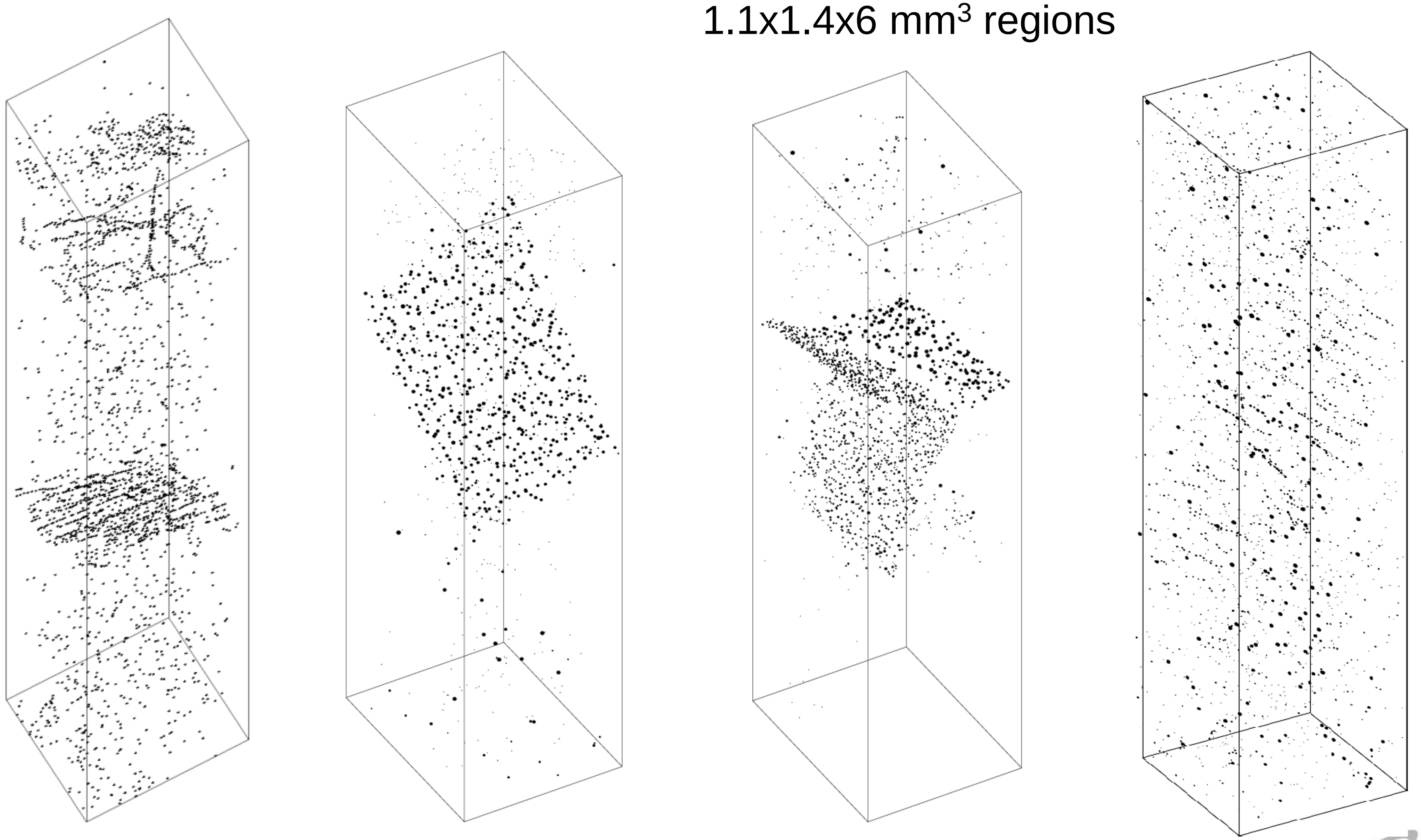

Roles of “small” and “big” defects

- “Small” defects (Te inclusions, low dislocation density boundaries):
  - Trap small amounts of charge from the electron cloud
  - Such defects cause random noise due to random distribution of interaction point => degrade energy resolution
  - Since the defect locations are fixed, they effects can be corrected by <u>segmenting the detector</u>
- “Big” defects (high dislocation density subgrain boundaries)
  - Trap significant amount of charge (incomplete charge collection events)
  - Cannot be corrected but can be identified and rejected

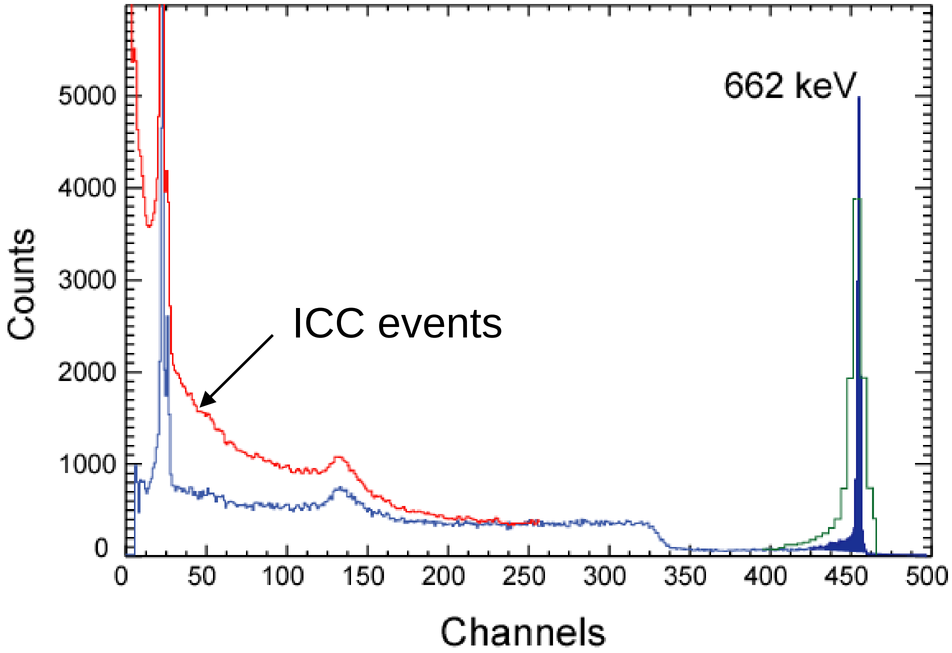

Operation principle of CZT detectors

- Single-type carrier device => suffer from the induction effect (i.e., amplitude dependence on interaction points locations)

Artist's view of a generalized CZT detector

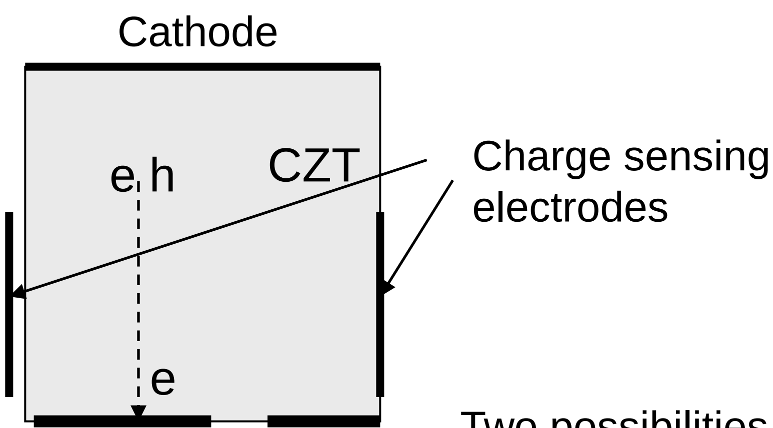

Charge collecting electrodes (anodes)

Induction effect

$$A_{out} \sim Q_{col} + Q_{ind}(x,y,z)$$

How to eliminate this term

Two possibilities to min ionization effect:

(1) Electrostatic shielding: Frisch-grid ionization chambers or virtual Frisch-grid CZT detectors (pixelated detector operates as a virtual Frisch-grid device)

(2) Subtracting holes signal: CPG

CZT detector designs

Out of many detector designs only two can practically mitigate nonuniformity problem of CZT material: Pixelated and arrays of virtual Frisch grid

Pixelated detector

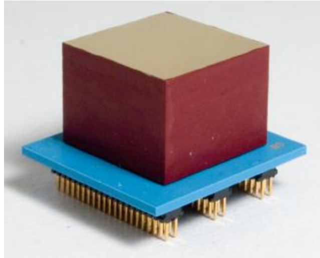

Virtual Frisch-grid detector

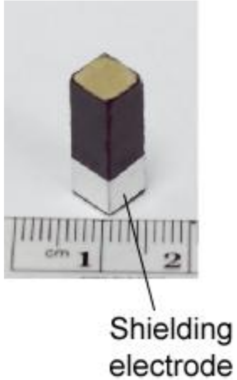

CPG detector is less promising

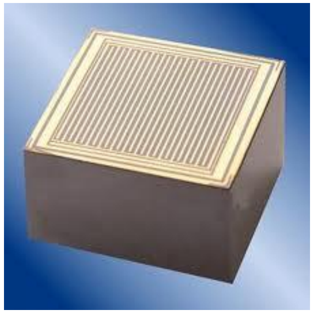

All these devices mimic their counterparts originally used for gas ionization chambers

Pixelated detectors and virtual Frisch-grid arrays are two competing technologies

Arrays of virtual Frisch-grid detectors

- Joint efforts (NNS and Instrumentation Division)
- The goal is to develop an array of virtual Frisch-grid detectors that can be used in hand-held and portable devices for imaging and spectroscopy of gamma rays
- Applications: nonproliferation and national security, dosimetry, geological survey, astrophysics
- The arrays have performance approaching that of 3D pixel detectors, but at lower cost and more suitable to the current supply of CZT crystals
- The current array consists of bar-shaped crystals; each crystal has a 6x6-mm^2 area and 15-mm length
- Bigger crystals can also be used; we tried in the past 7x7x20 mm^3

Large area detecting plane coupled with a coded aperture mask for long-range detections

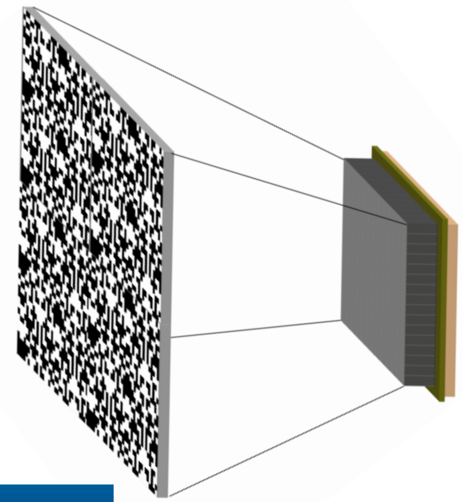

Portable, battery-powered device

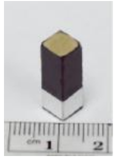

Array of virtual Frisch-grid detectors Vs. pixel detector

- The overall energy resolution of less than 1.3% at 662 keV which is adequate to resolve the majority of gamma-ray lines
- 6 mm position resolution in XY and < 1 mm in Z is suitable for coded aperture telescopes
- The detection sensitivity (the most critical parameter for security-related application) scales as:

$$I \sim \frac{\sqrt{\Delta E}}{S_{eff}}$$

- 1.3% is ~2 times greater than typical resolution of 3D detectors (0.6%), which gives a 1.4 factor of sensitivity loss; it can be compensated by making larger-area detectors
- The relaxed requirements to the energy resolution means that crystals with defects can be used; such crystals can be supplied at lower cost
- Benefits of the crystal geometry (easy to cut from wafers, easy to screen, and higher yield)

Improvements in virtual Frisch-grid detector designs

This technology has come a long way

CAPture (eV Product)

Frisch-Ring and capacitive Frisch-ring (D. McGregor et al. and G. Montemont et al., LETI.)

BNL design

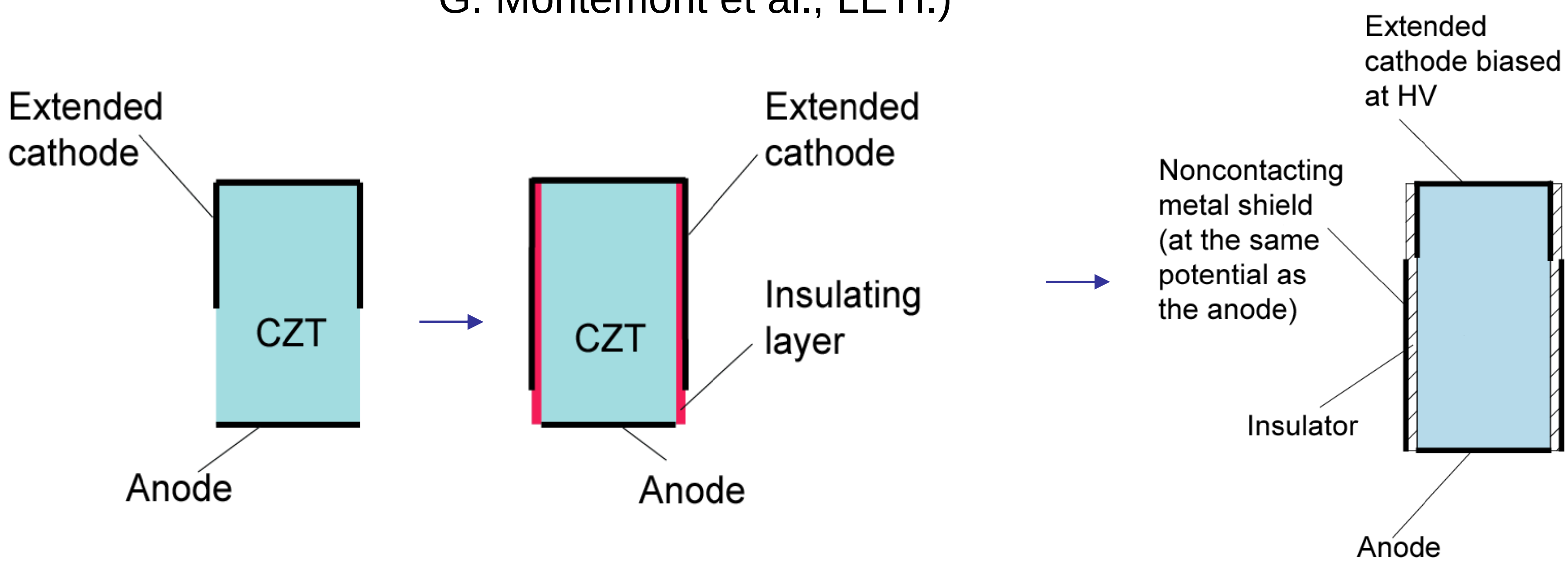

Critical drawback: the cathode is also shielded (as the anode) and cannot be used for sensing interaction depth or drift time measurements

Our new design

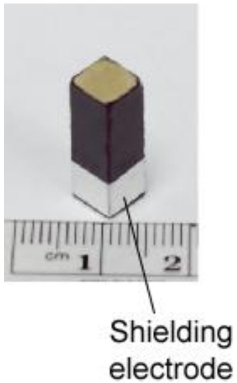

(1) Long detectors - up to 20 mm. This allows us to:

- Use a narrow (~5-mm wide) shielding electrode placed near the anode without compromising the anode shielding

(2) Connect cathode of 2x2, 3x3 or even 4x4 detectors together to make a common cathode; use cathode signals to measure electron drift times and interaction depths to:

- Correct for the electron trapping
- Reject the incomplete charge collection events (ICC) including the events interacting near the anode (inside the collection region)

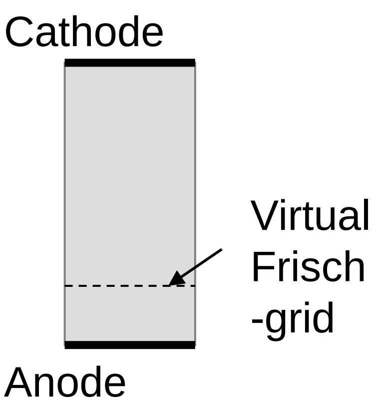

Schematic of the array

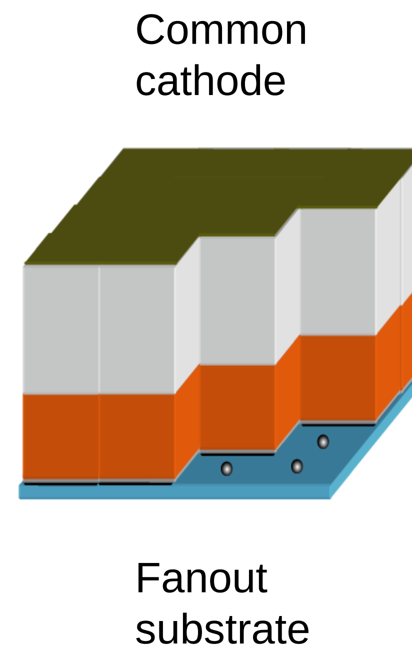

Virtual Frisch-grid detector is 100% analogous to the classic gas ionization chamber

Classic ionization chamber and virtual Frisch-grid detector (same scale)

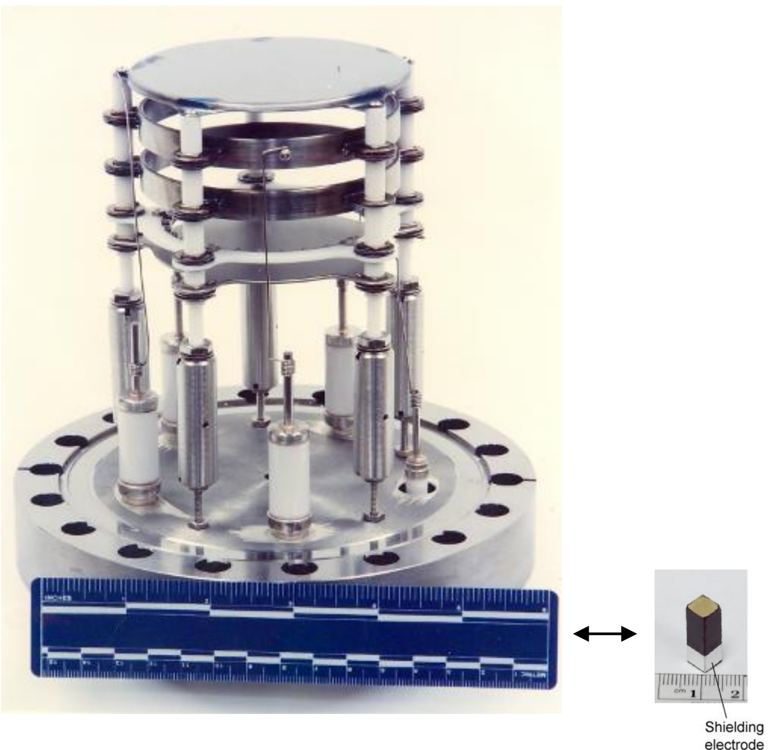

G. Smith, P. Vanier, and G. Mahler, BNL

Surface leakage current is important

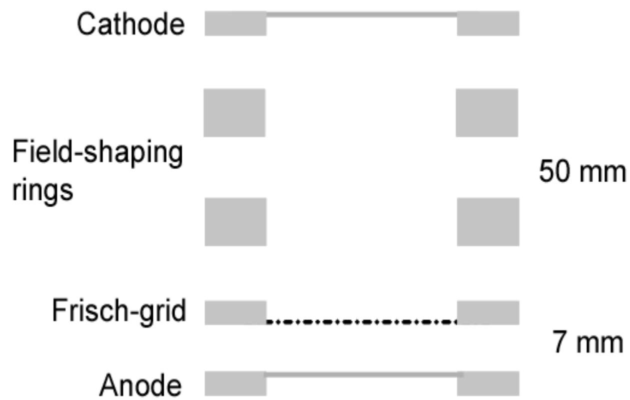

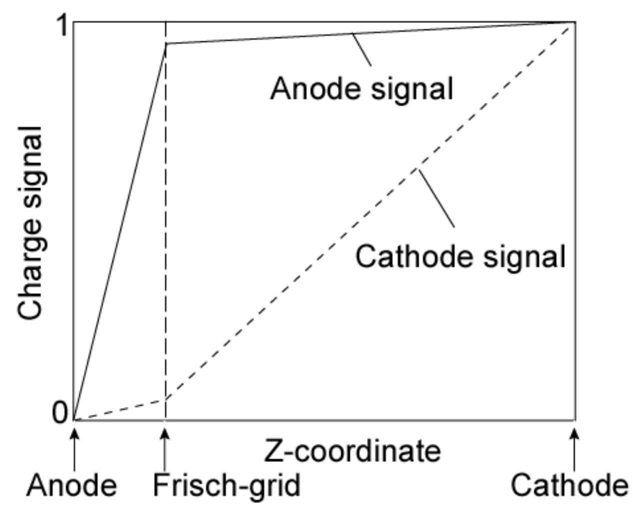

O. Buneman et el., Can. J. Res. **A27**, 191–206 (1949).

Dependencies *C vs. T, A vs. T, and C/A vs. T* simulated for 662 keV photons

6x6x15 mm^3 detector, 2000 V cathode bias, no charge trapping

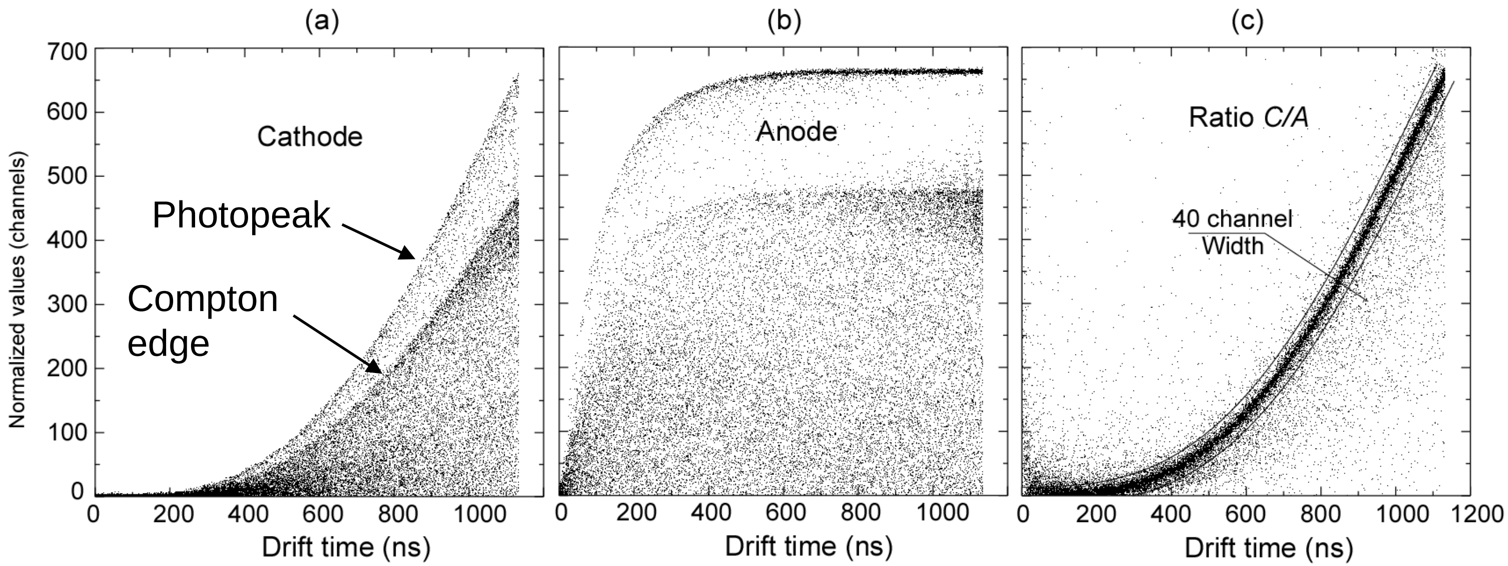

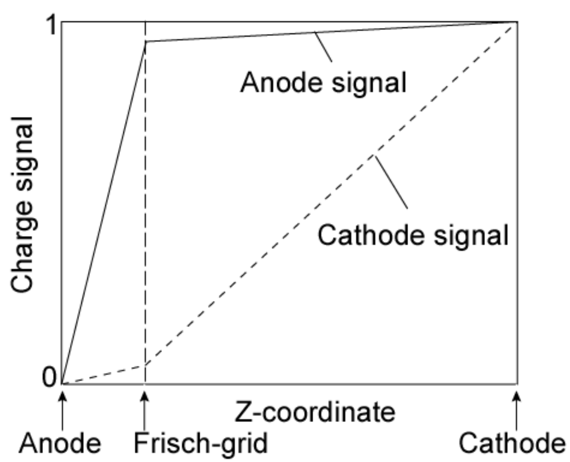

The ratio C/A is commonly used as a measure of drift time for single point interactions events

C/A can also be used for rejection of the incomplete charge collection events! This is a new feature we proposed for virtual Frisch-grid detectors!

Measured response from the 6x6x15 mm^3 virtual Frisch-detector

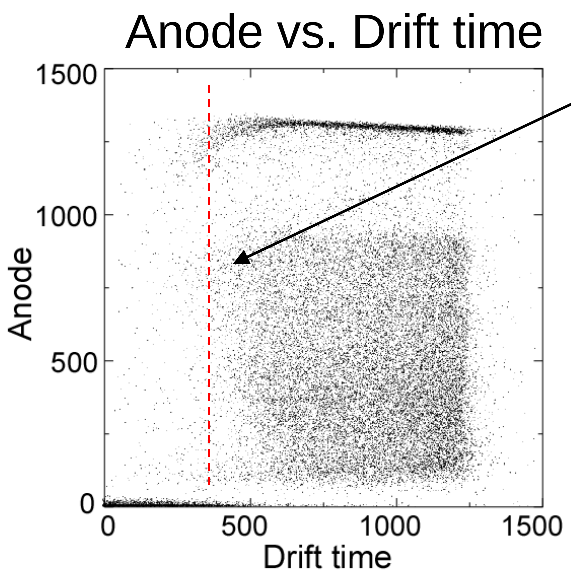

Position of the virtual Frisch grid

Nearly constant response from the drift region

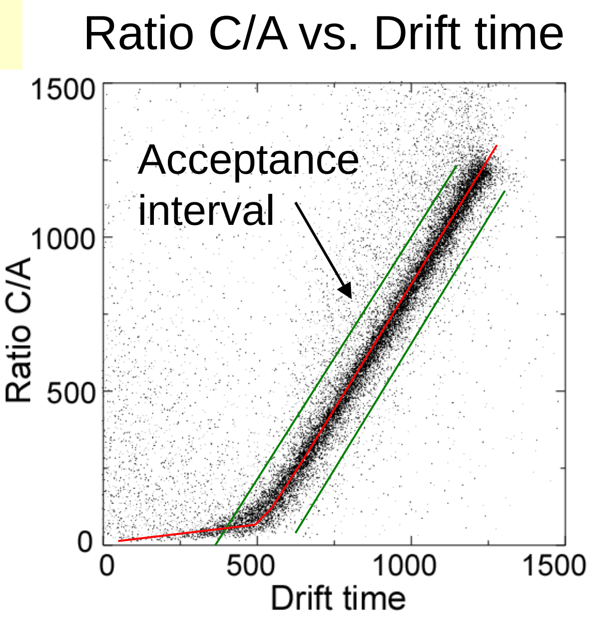

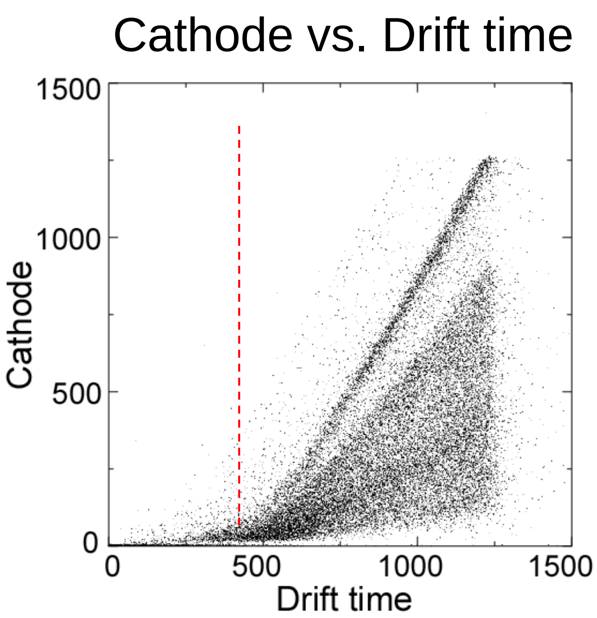

Almost linear response from the drift region

C/A vs. T is used to reject the ICC events. The red curve is a cathode signal induced by a unit charge vs. drift time

Br
U.

Examples of spectral improvements by rejection of ICC events

ICC events cased by crystal defects and charge trapping at the edges

Two 15-mm long virtual Frisch-grid detectors with different contents of defects

Rejection does not affect the photopeaks

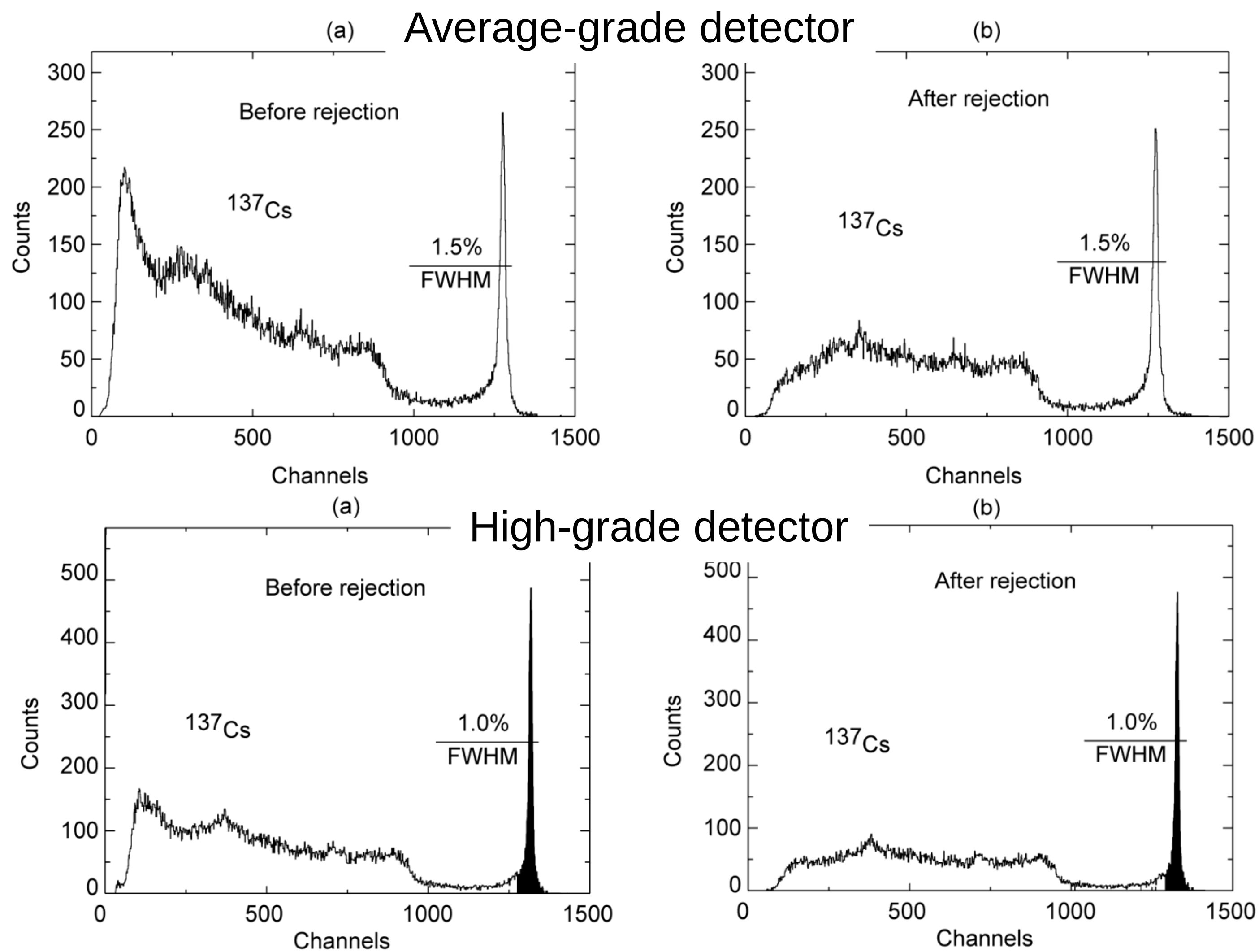

BROOKHAVEN NATIONAL LABORATORY

Future improvements: segmentation

Position sensitive virtual Frisch-grid detector

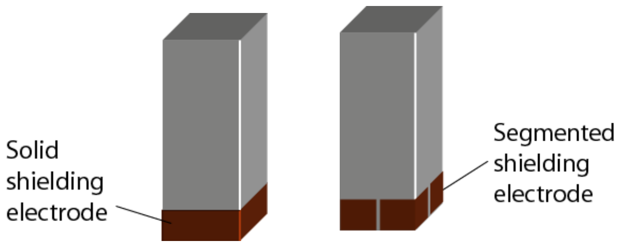

- Very preliminary results from 6x6x15 mm^3 average grade detector: each spectrum corresponds to 0.6x0.6 mm^3 area
- No charge sharing complications!
- Suspiciously good results: events interacting close to the anode could be lost?
- For comparison, 3D pixelated detector has 1.9-mm pitch

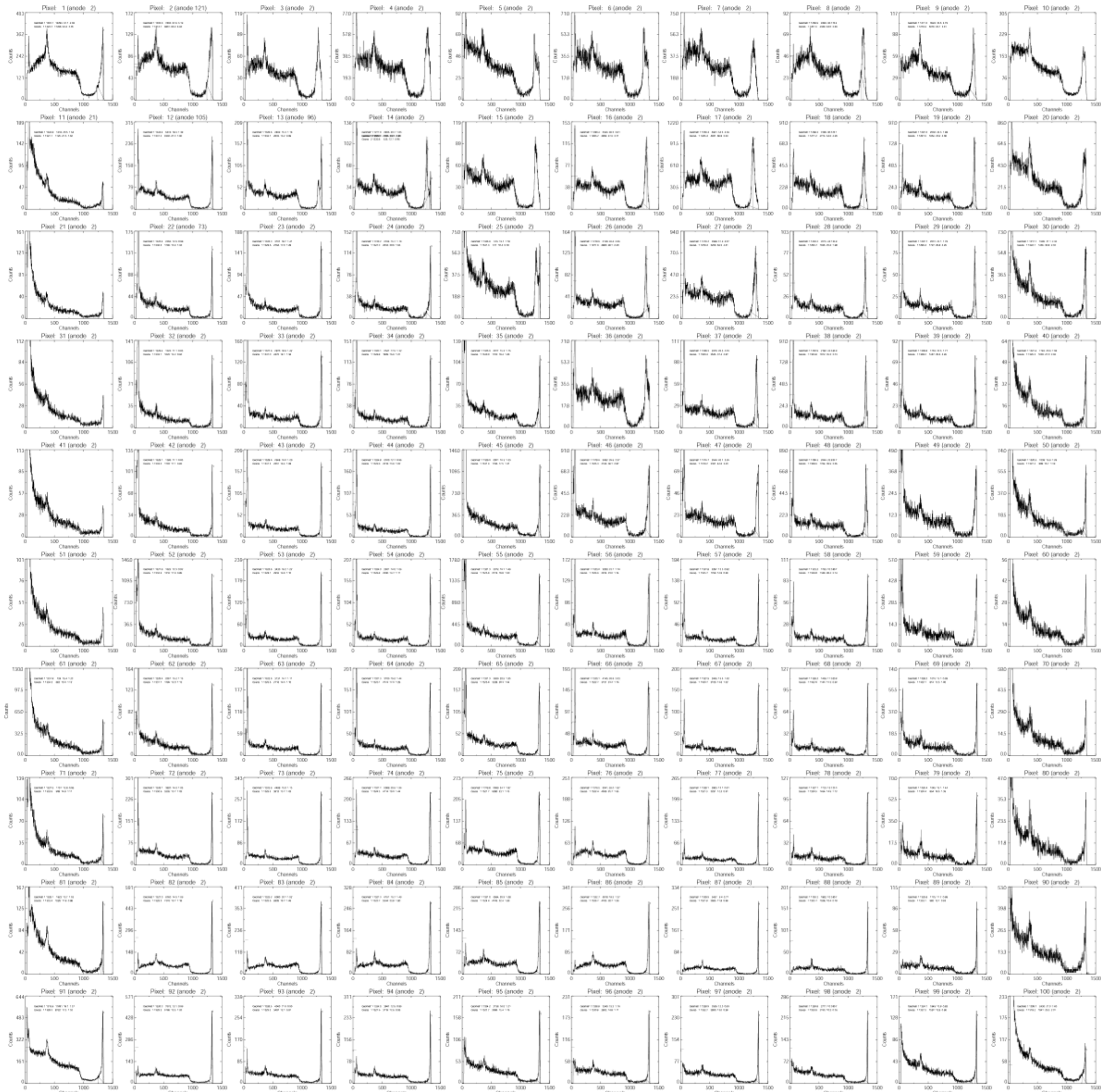

Fabrication and testing of individual detectors

For insulation and mechanical protection of CZT crystals, we use the ultra-thin polyester shrink tube (Advanced Polymer, Inc.)

This material has very high dielectric strength and resistivity

Dielectric strength: > 4,000 V/mil
Volume Resistivity: 10^{18} Ohm-cm,
Surface Resistivity: 10^{14} Ohm/square,
Dielectric Constant: 3.3

A crystal and two aluminum bars are inserted inside the tube and put inside hot water (~80 C) for 2-3 min. The remaining tube is cut and edges are trimmed.

A layer of aluminum or copper tape is then placed around the detector.

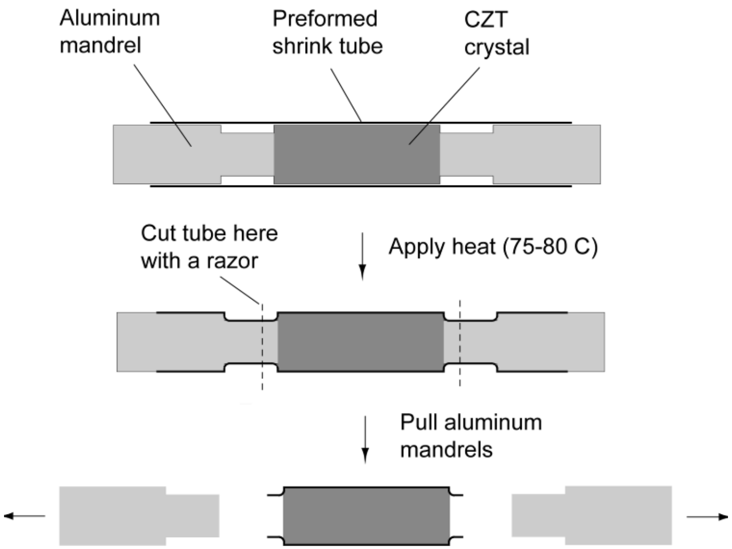

Testing of individual detectors

Coincidence set up for testing virtual Frisch-grid detectors

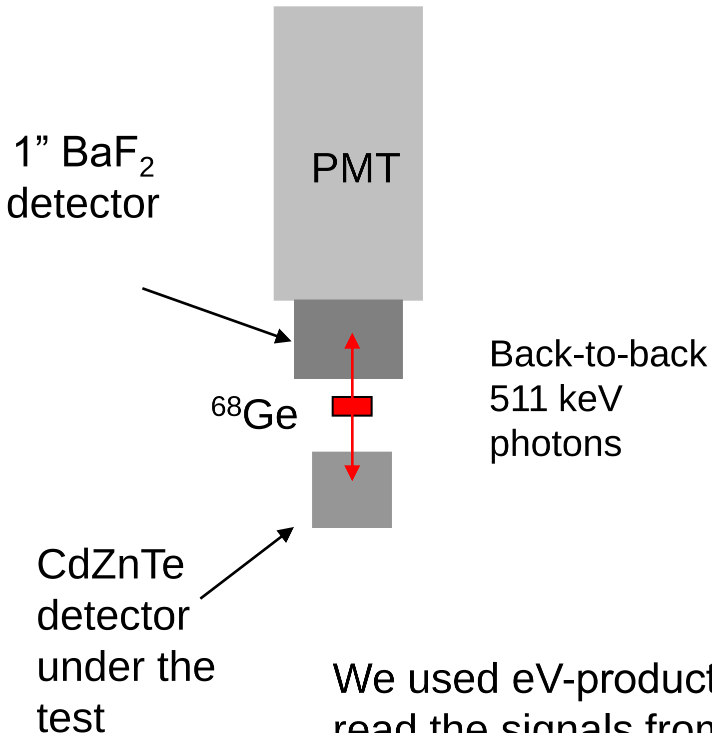

Typical waveform from a 15-mm-long virtual Frisch-grid detector

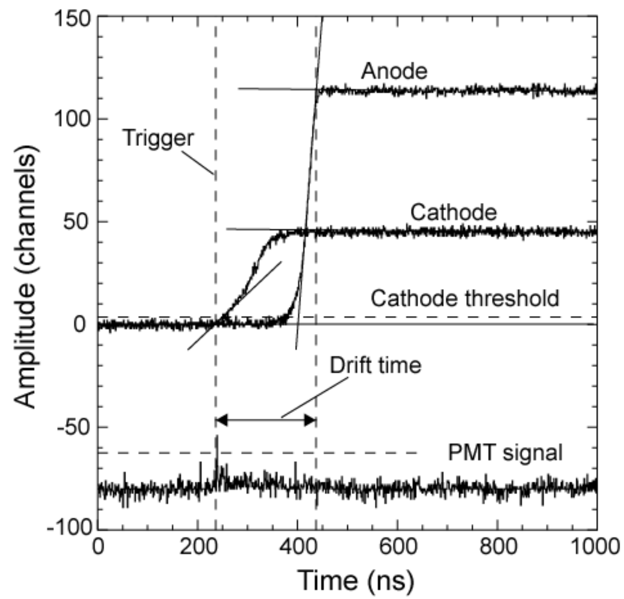

We used eV-product’s hybrid preamplifiers to read the signals from the anode and the cathode

Position of the virtual Frisch-grid depends on the location and width of the shielding electrode

Anode amplitude vs. drift time

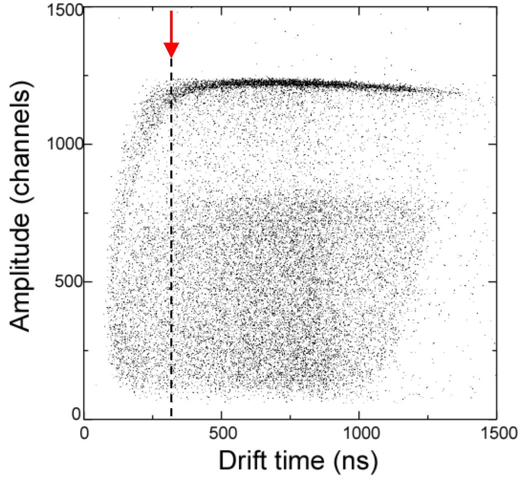

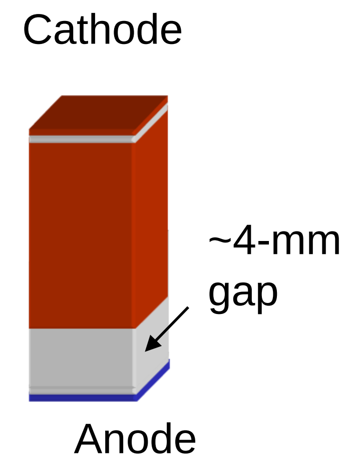

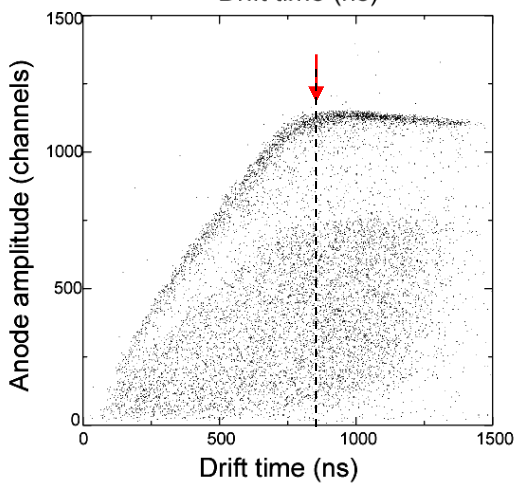

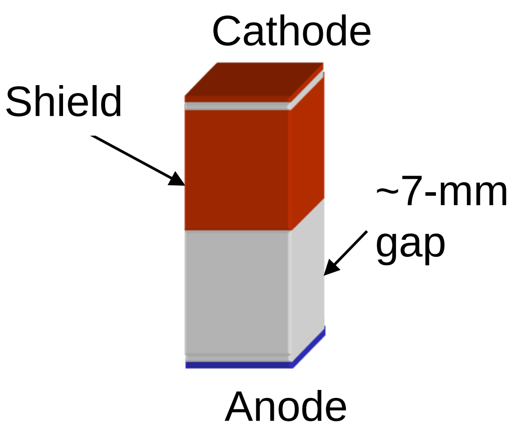

Shielding electrode must be close to the anode

BROOKHAVEN
NATIONAL LABORATORY

Finding optimal width of the shielding electrode

$6x6x15\ mm^3$ crystals

Optimal length: 5 mm

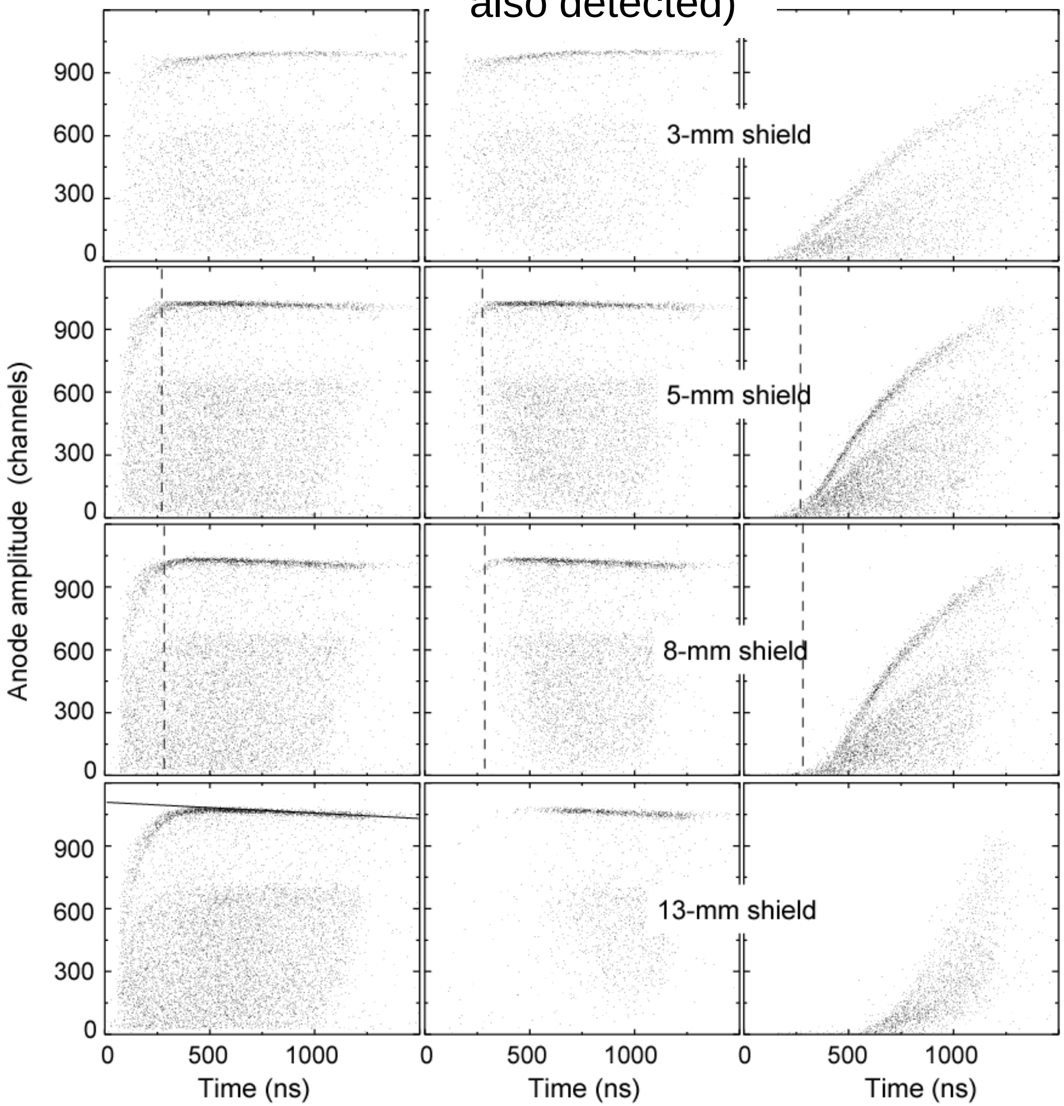

BROOKHAVEN NATIONAL LABORATORY

Feasibility studies: results from a 2x2 array prototype

- Demonstrated a feasibility of 2x2 array of 6x6x15 mm^3 virtual Frisch-grid detectors with the common cathode
- 4 detectors were mounted on the substrate with connectors matching the 3D readout system

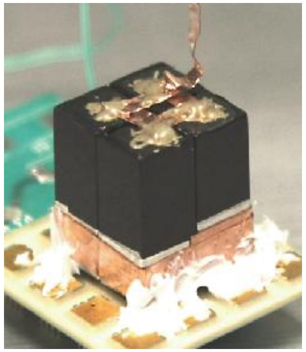

Test box containing readout electronics based on the H3D ASIC developed by BNL's Instrumentation Division and University of Michigan

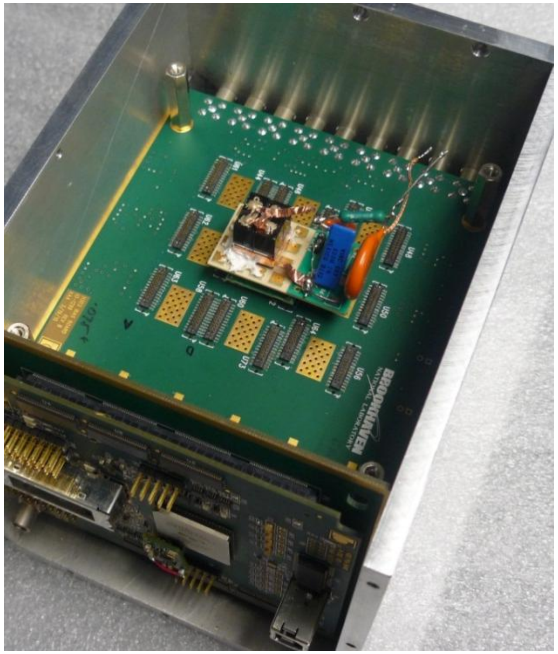

Pulse-height spectra measured from 4 detectors

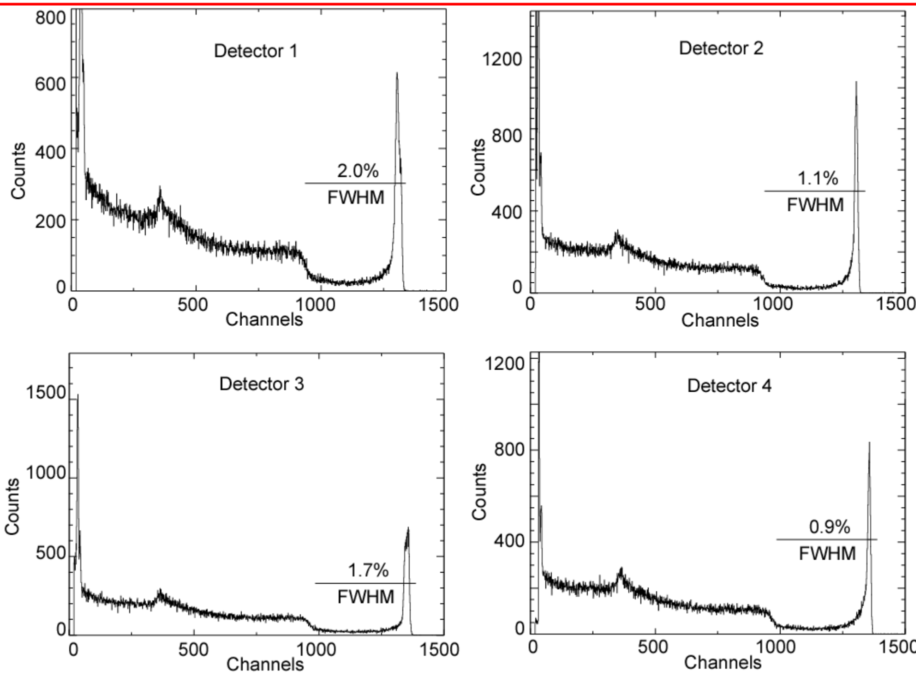

Raw spectra

Spectra after the charge-loss correction

Good energy resolution
Large peak-to-Compton ratio

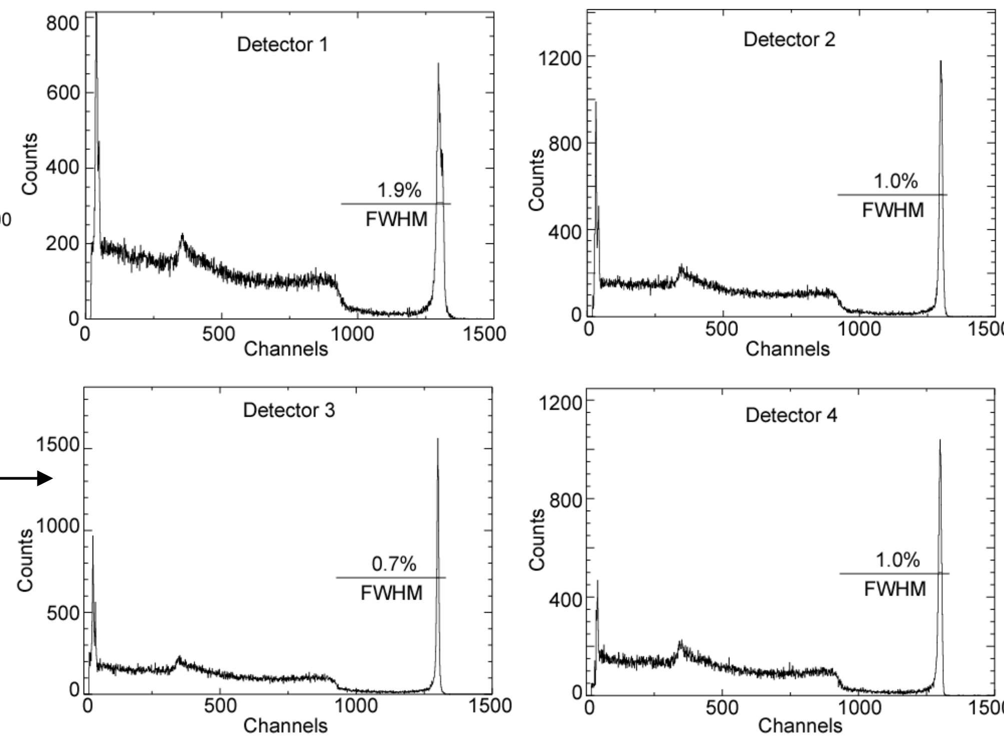

Combined spectra from all detectors

All detected events
(without adding the signals)

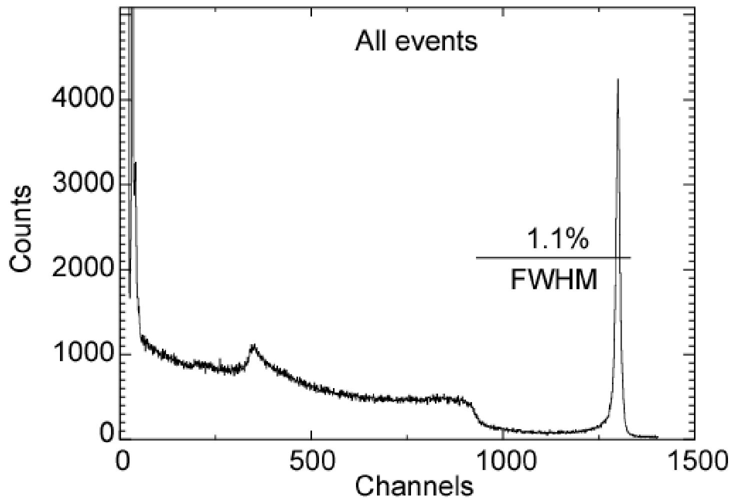

Single-detector events

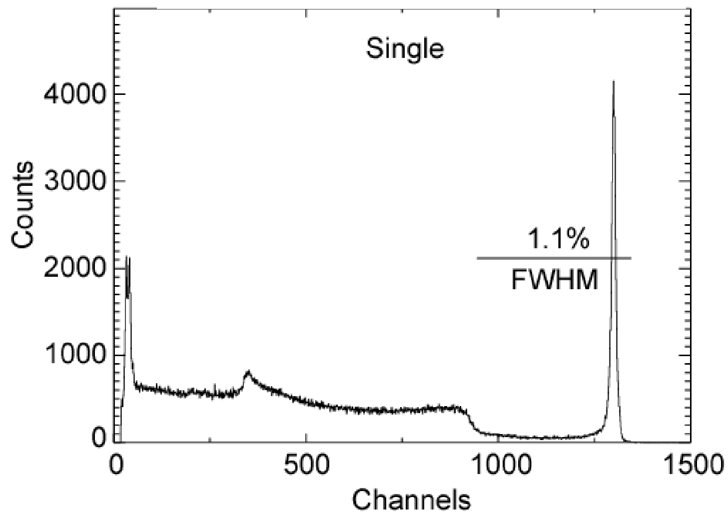

Two-detector events

Signals from two detectors are added together

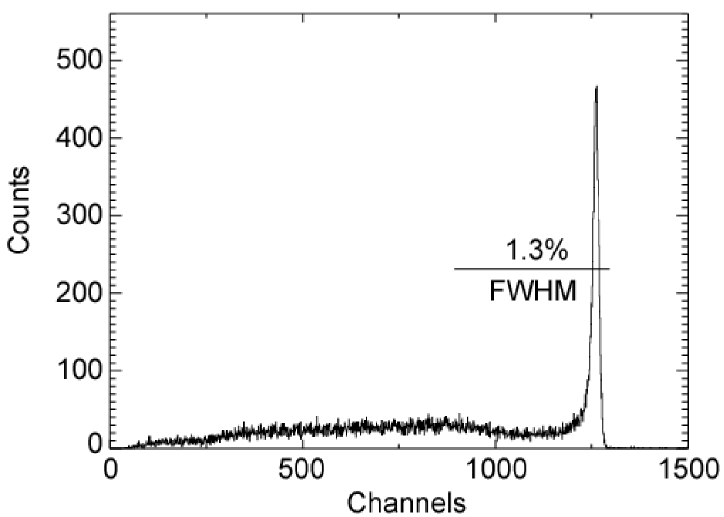

Better energy resolution, < 1%, can be achieved by selecting crystals with better quality which are more expensive

However, <1.3% requirement will allow us to use unselected, readily available and less-expensive crystals

BROOKHAVEN NATIONAL LABORATORY

Schematic of the array's design

12x12 detector array
Detectors are grouped in smaller sub-arrays
Design and fabricated new ASIC: 32 anodes, 8 cathode

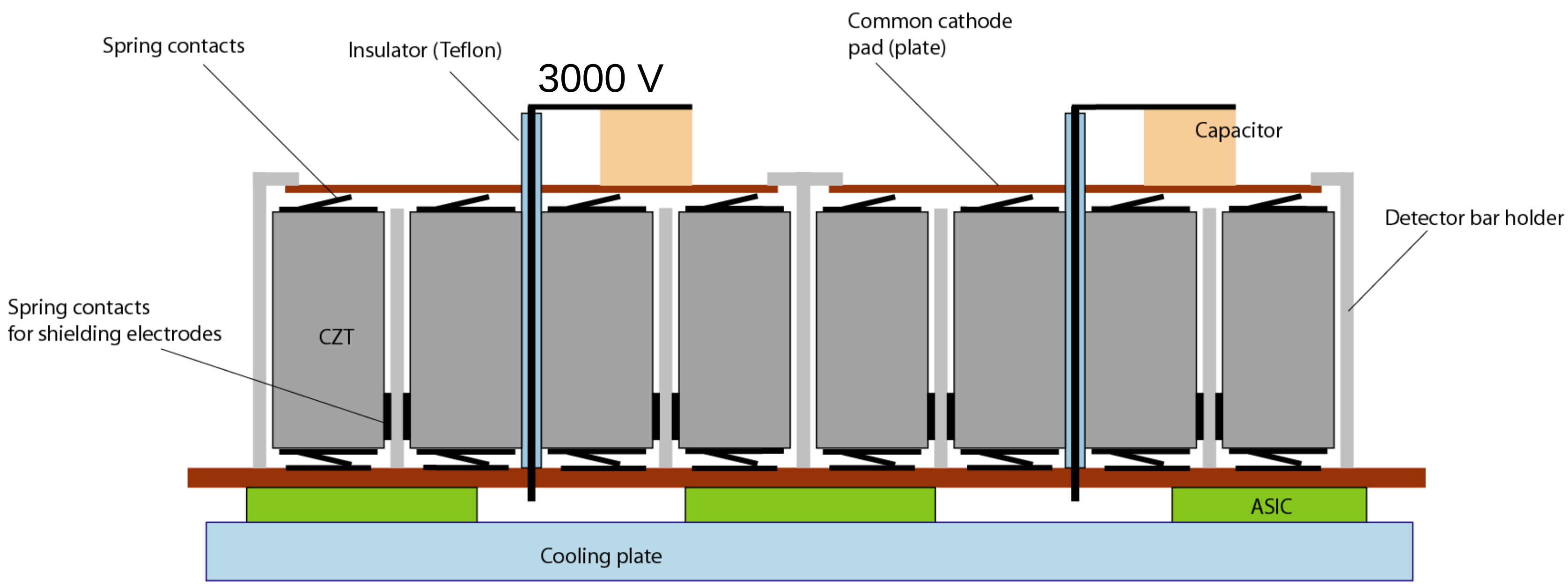

Schematic of the array design (example of a 2x2 sub-array with a common cathode)

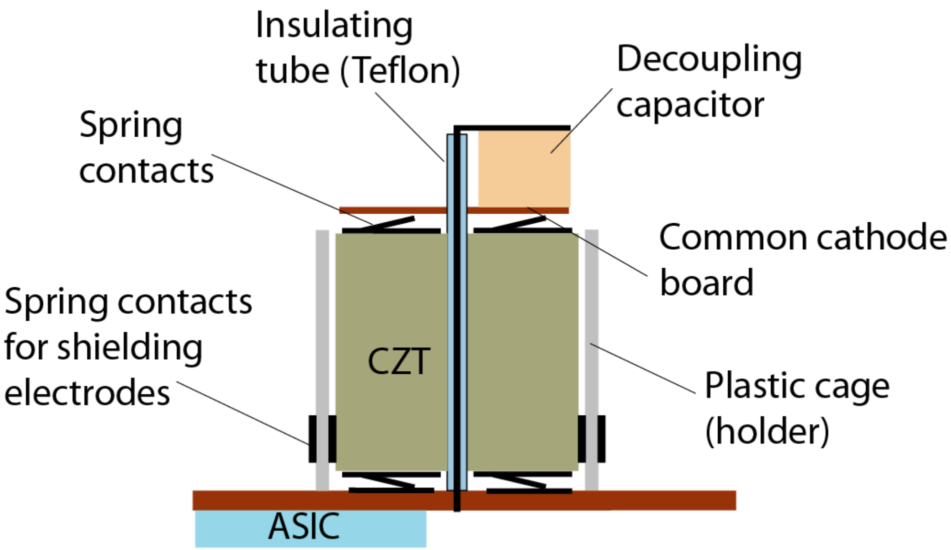

This example shows detectors grouped in 2x2 sub-arrays with the common cathodes

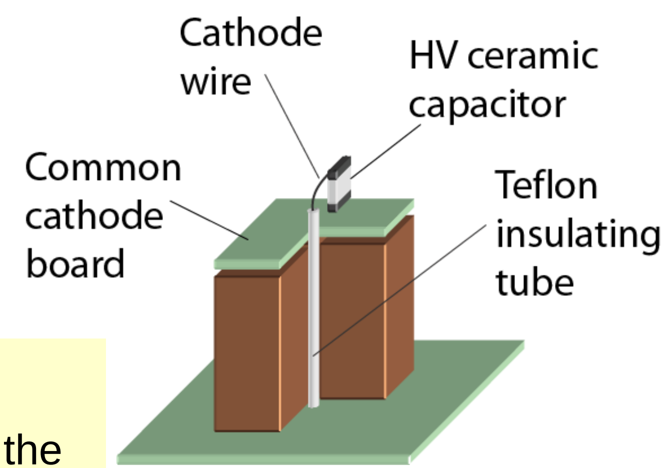

ASIC:32 anodes and 8 cathodes

Questions regarding to this design:

- Evaluated possible interferences (cross-talk) between the anodes and cathodes' wires and between the adjacent cathodes
- Evaluated reliability of the spring contacts
- Completed the HV test of the material used for fabrication of the holder

Detectors used in these measurements

- For these measurements we used 9 6x6x15 cm^3 detectors, supplied by Endicott Interconnect and Redlen
- The quality of these detectors is rated 3 and 4 on a scale of 1 to 5

Criteria of crystal rating

Rate	Spectral features
5	No response degradation
3-4	Have good energy resolution, <1.5%, but elevated low-energy continuum due to incomplete charge collection (ICC) events
1-2	Usable because of either the high leakage current or lack of spectral response

Leakage currents map (nA) measured for the 3x3 array at -2500 V

3.6	3.8	4.1
9.8	5.6	4.2
5.5	4.9	7.4

ASIC can handle the cathode leakage current up to 100 nA => the 4x4 array can potentially be used as a single cathode

Example of the high-grade detector

Micro-scale resolution
X-ray response map

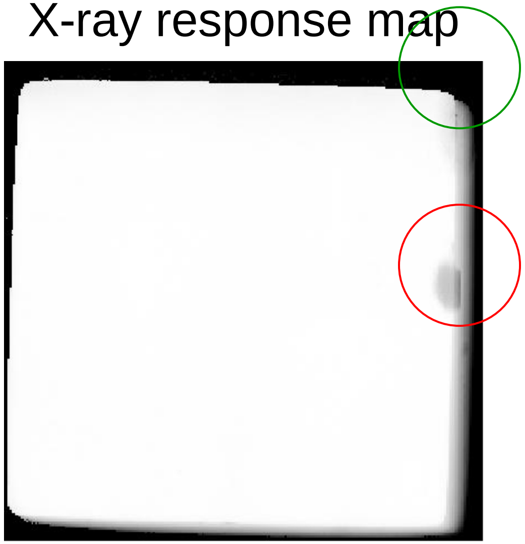

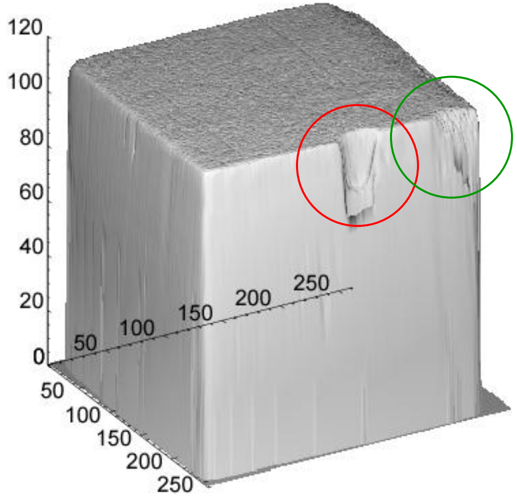

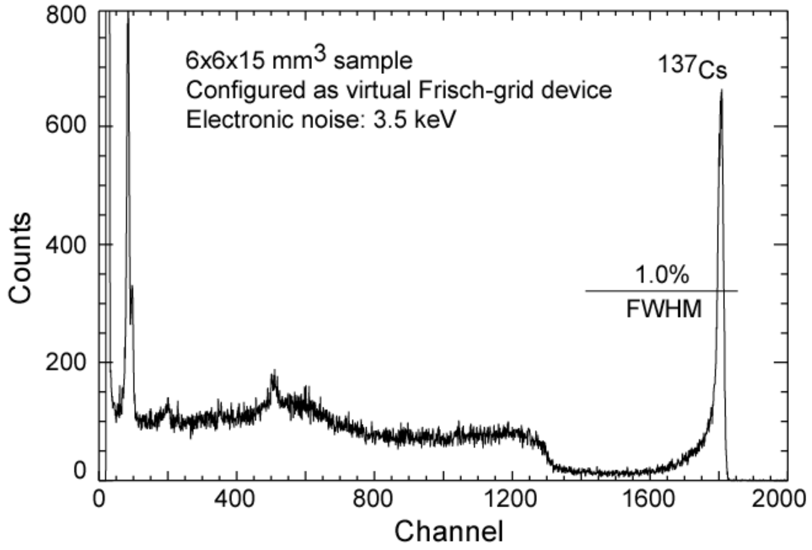

X-ray diffraction topograph

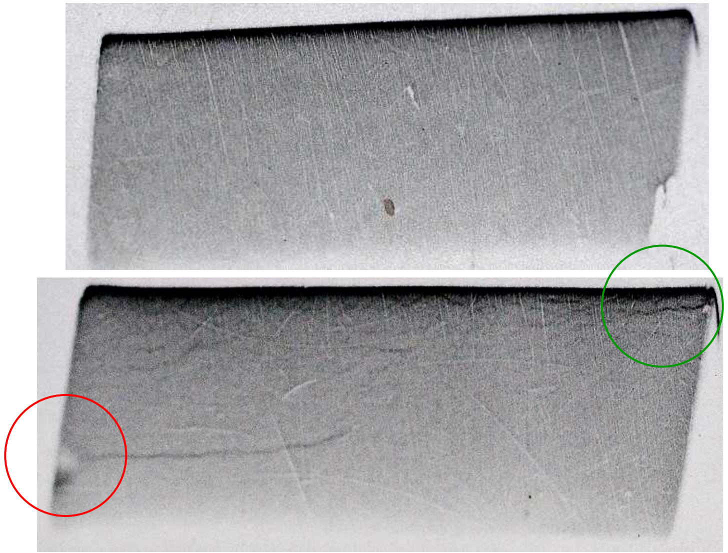

Average-grade (rating 3-4) detector

X-ray response map

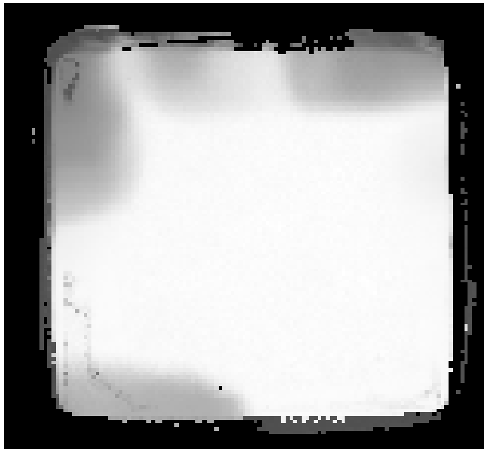

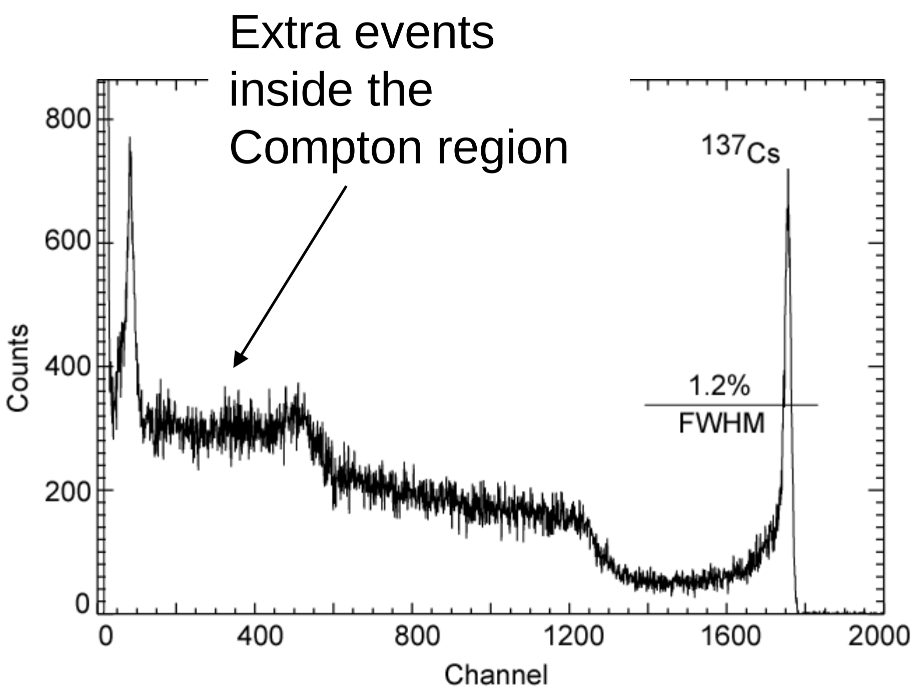

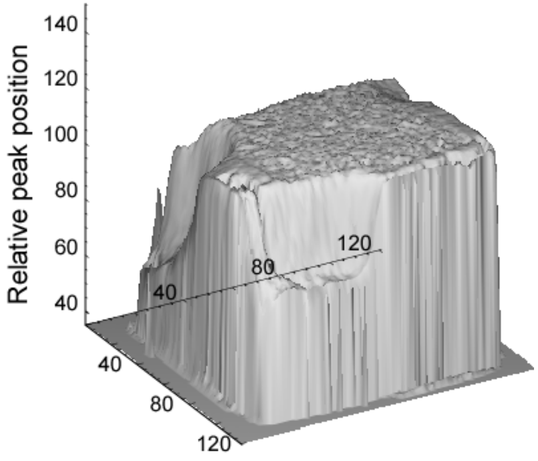

Average grade detectors show energy spectra with reduced photopeak efficiency and larger fraction of low-energy events the Compton region

Example of a low-grade (unusable) detector

X-ray raster scan

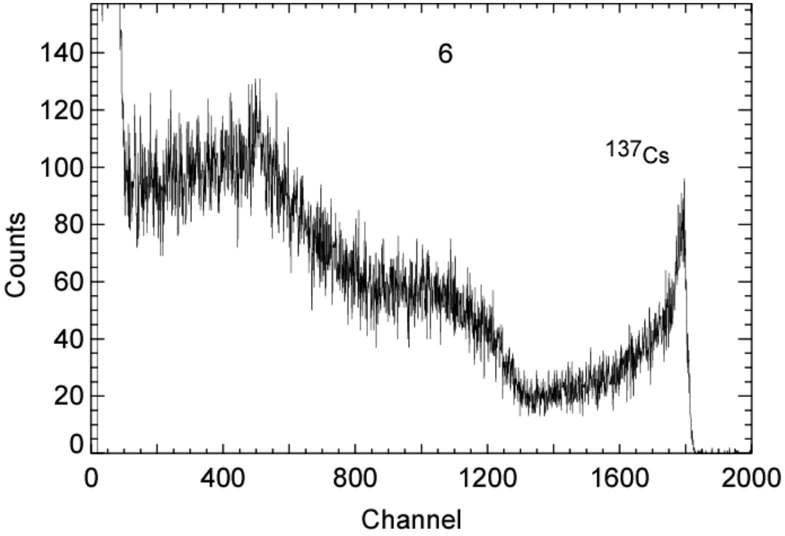

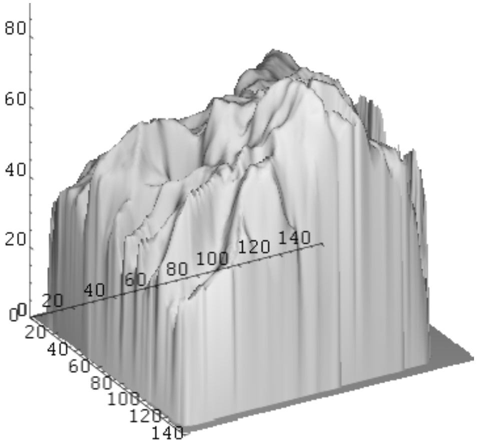

X-ray diffraction topograph

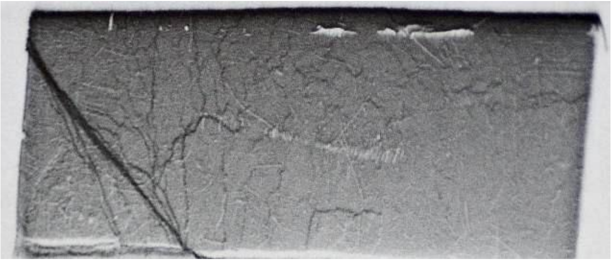

Diffraction topography data reveal large number of subgrain boundaries

BROOKHAVEN NATIONAL LABORATORY

Detectors and array-assembling steps

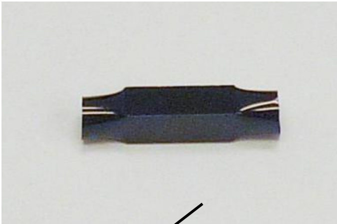

Detector encapsulated inside a thin polyester shell

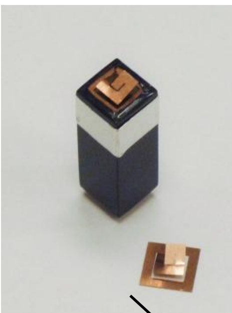

Assembled detector with two spring-loaded contacts

Array mounted on a substrate

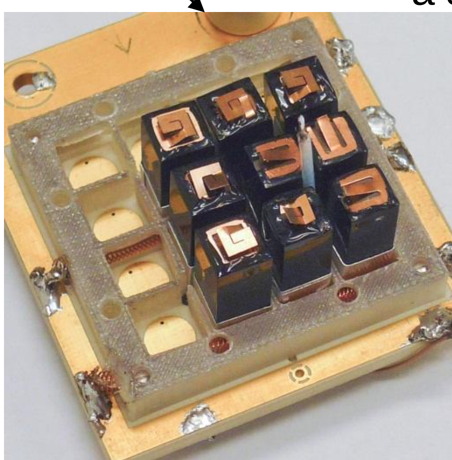

Test box containing readout electronics and connectors for evaluating pixel detectors or arrays

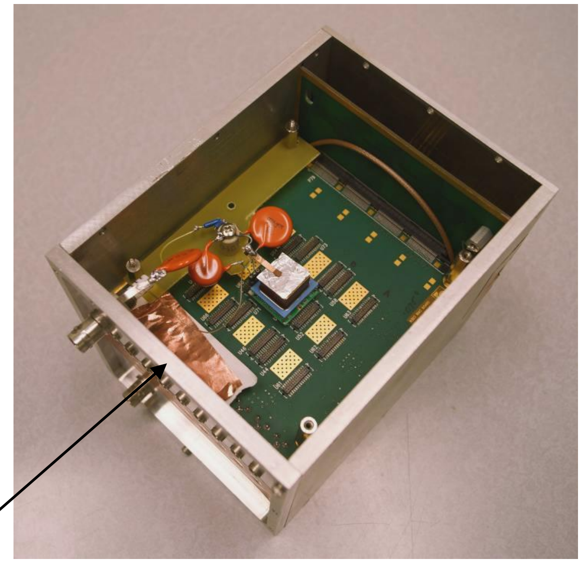

We could easily rearrange the detectors for making 2x2, 2x4, 3x3 and 4x4 arrays

Cathode bias: 2500 V; cathode and anode peaking time: 1 μs

Cooling is important: we use an environmental chamber to stabilize the temperature at 18 C

Results from testing of 2x4 array with two common cathodes: Spectra from ^{137}Cs source

2x4 array with two common cathodes

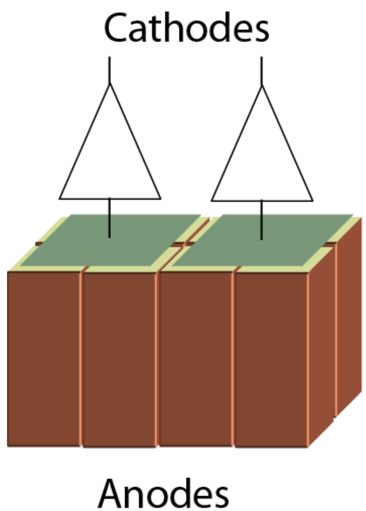

After charge-loss correction

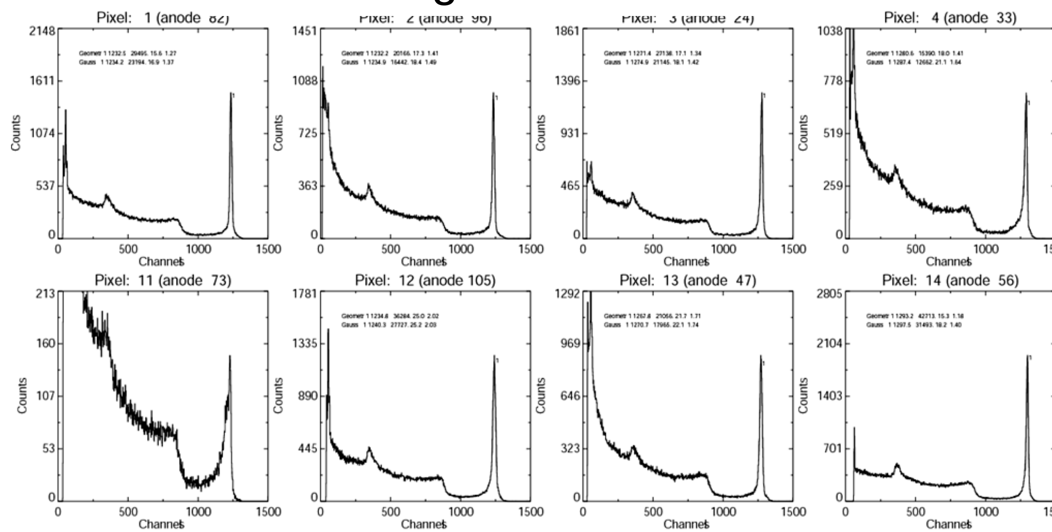

After rejecting ICC events

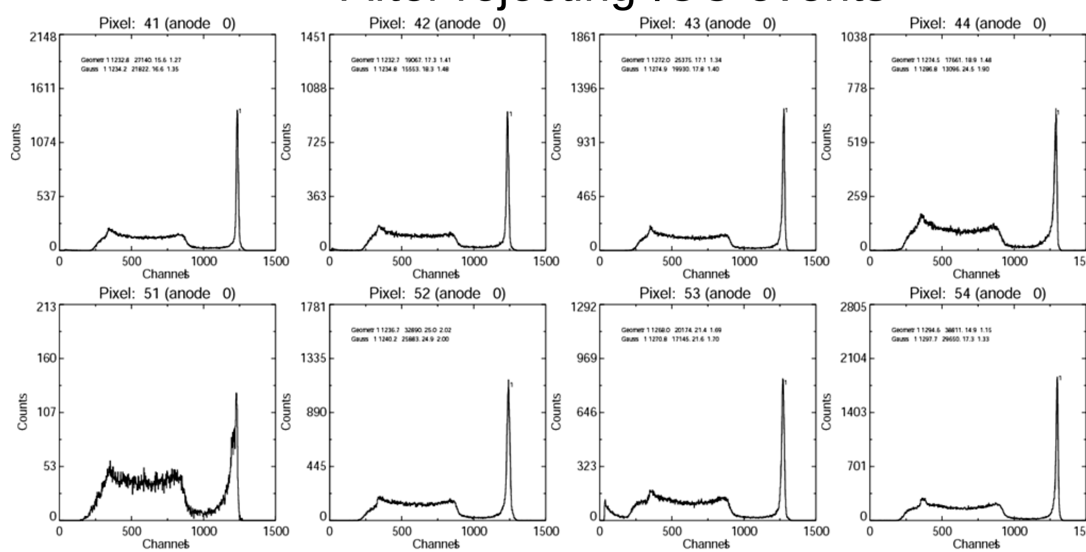

No interference between the cathode wires and anodes and common cathodes

Energy resolution is in a range of 1.2-1.7% FWHM at 662 keV

Results from testing of 2x4 array with two common cathodes: Correlations between cathode signals

2x4 array with two common cathodes

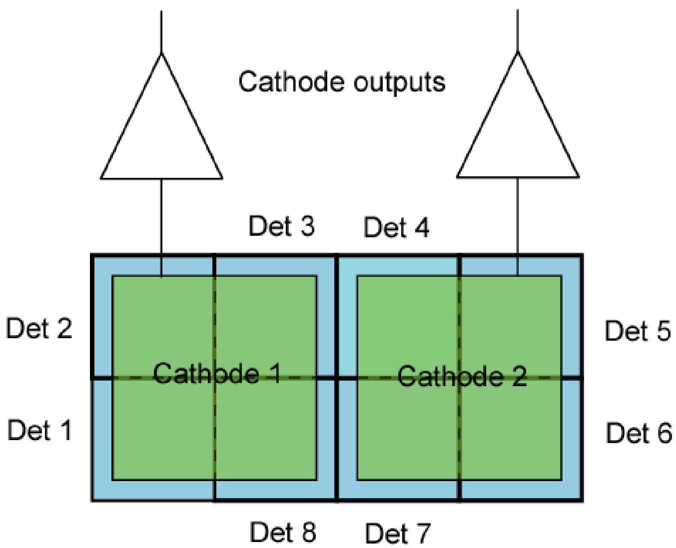

Use a ^{137}Cs source for these measurements

A small cross-talk is seen

Nevertheless, this has no effect on the performance!

All events

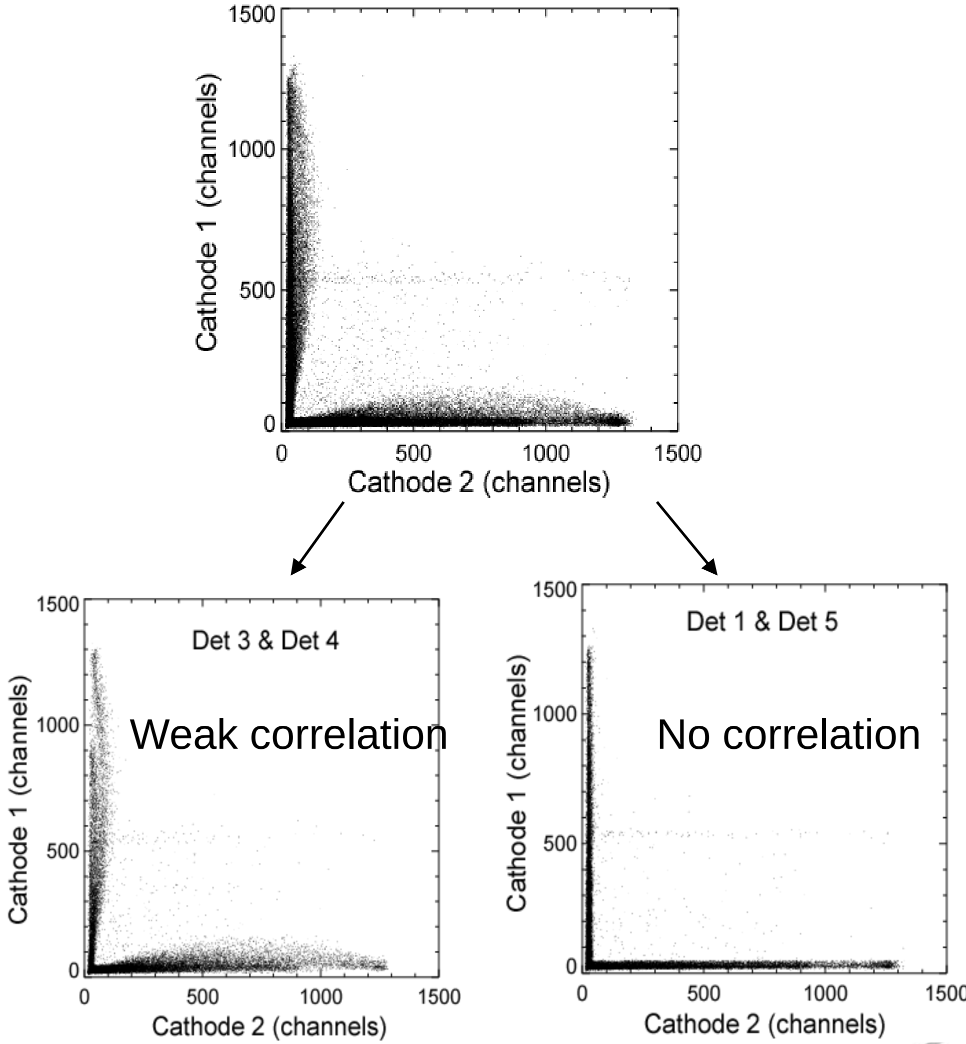

BROOKHAVEN NATIONAL LABORATORY

3x3 array: Illustration of charge–loss correction techniques

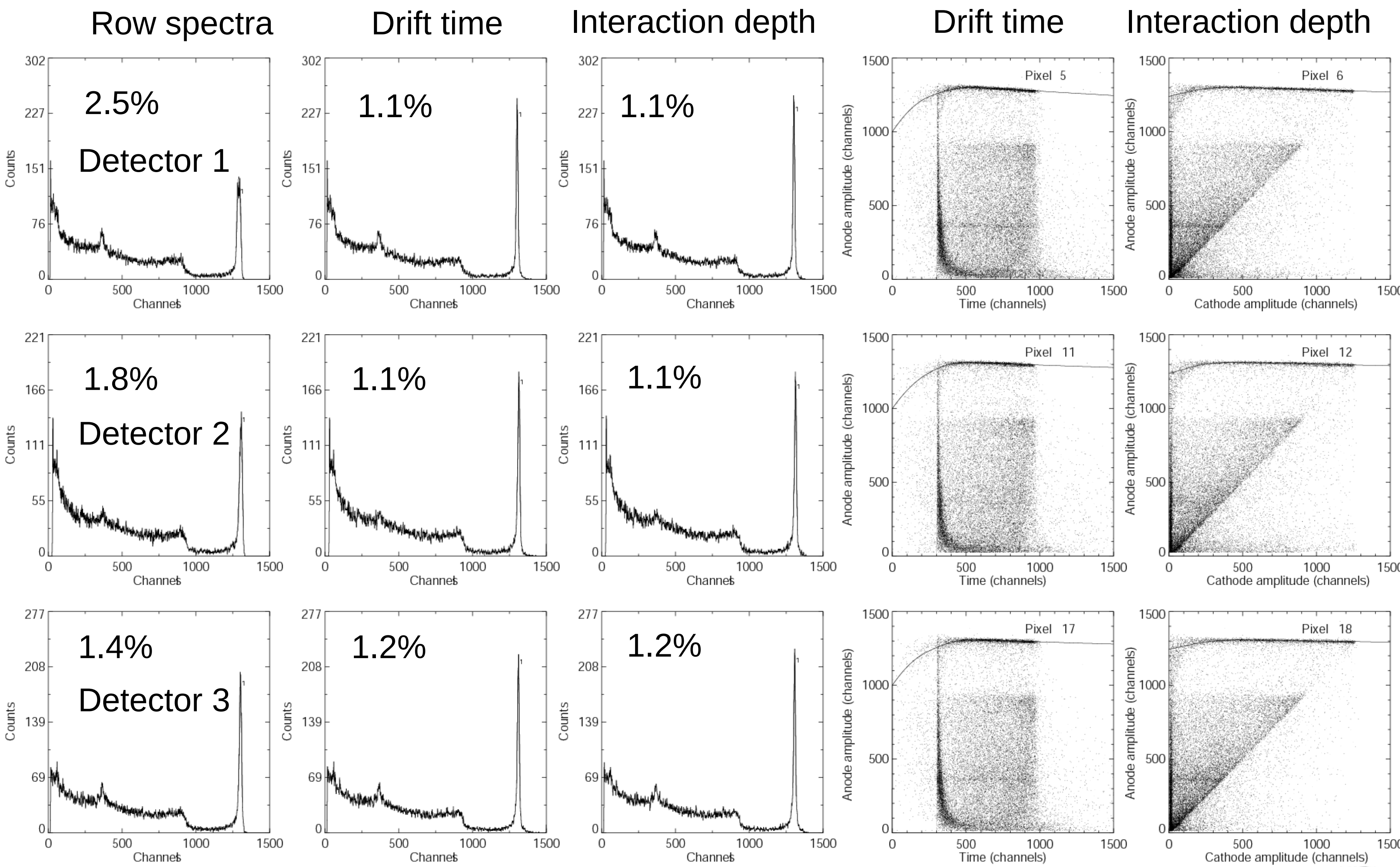

Numbers represent energy resolution, %FWHM at 662 keV

3x3 array: Rejecting ICC events (^{137}Cs) for three selected detectors (single detectors events)

Original spectra | Accepted | Rejected | Events distribution in *R vs. t* space

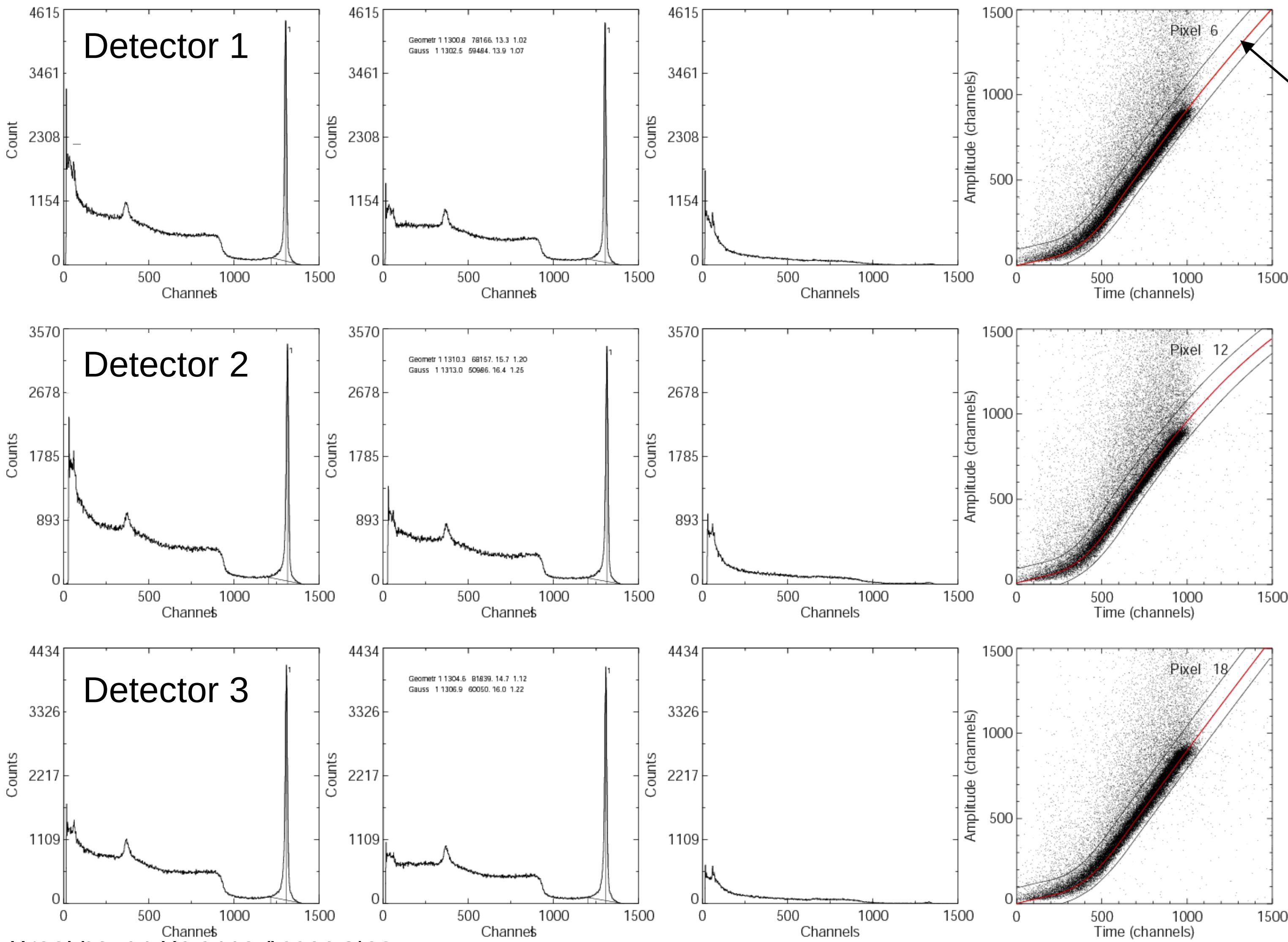

The correlation function *is* defined as a ratio

R(t)=C/A

It was evaluated selecting the photopeak events (^{137}Cs source) and potting them as *C/A vs. t.*

Applied soft rejection constraints

Results from testing a 3x3 array: Spectral responses from ^{137}Cs measured at 2500 V

Raw spectra

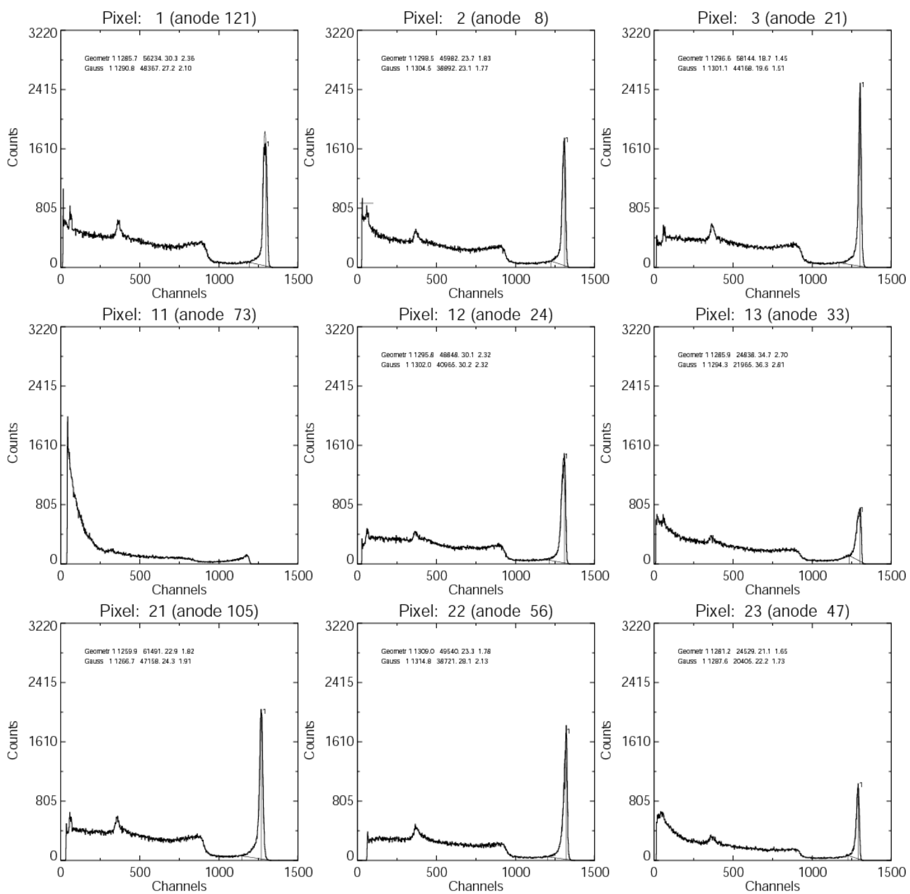

After charge-loss correction and rejecting ICC events

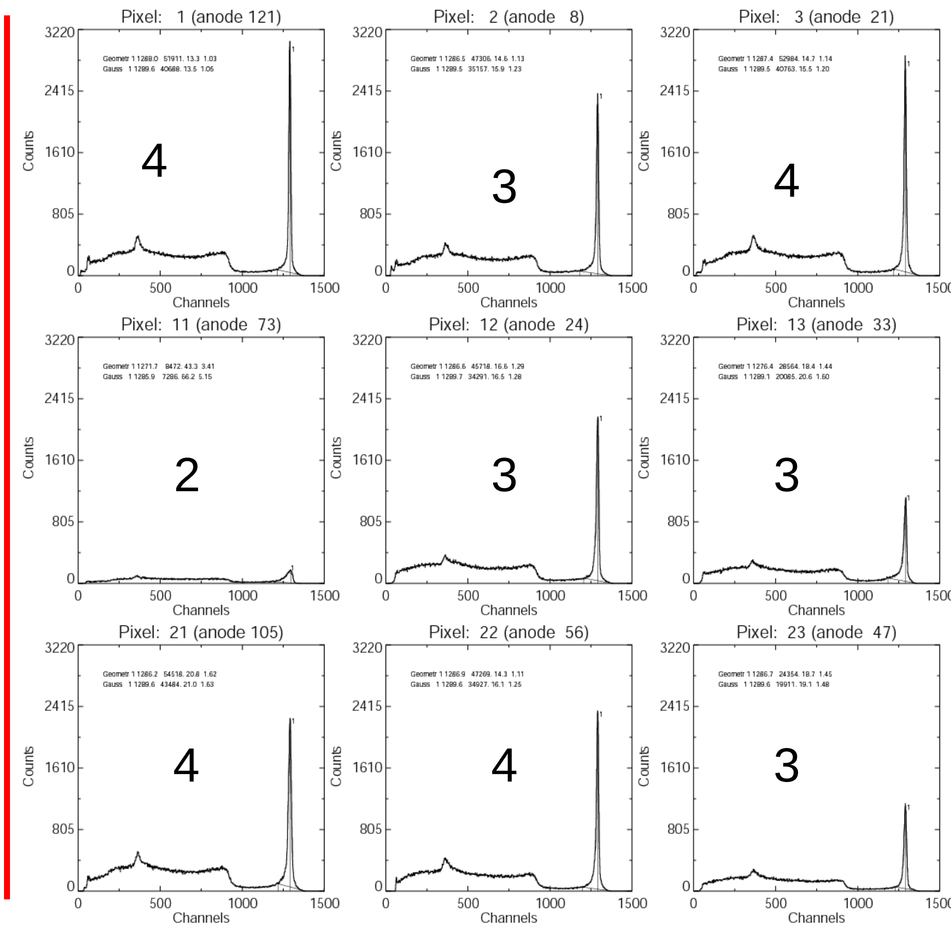

Here we use same scale for plotting all spectra (resolution is 1.2-1.5%)
Numbers indicate detectors' ratings.
Good response after corrections, but some detectors show reduced photo-peak efficiency

3x3 array: Single interaction events spectra after ICC rejection

Numbers indicates relative photopeak efficiency and energy resolution (FWHM) at 662 keV

Photoefficiency was evaluated on the basis of the number of events under the photopeaks

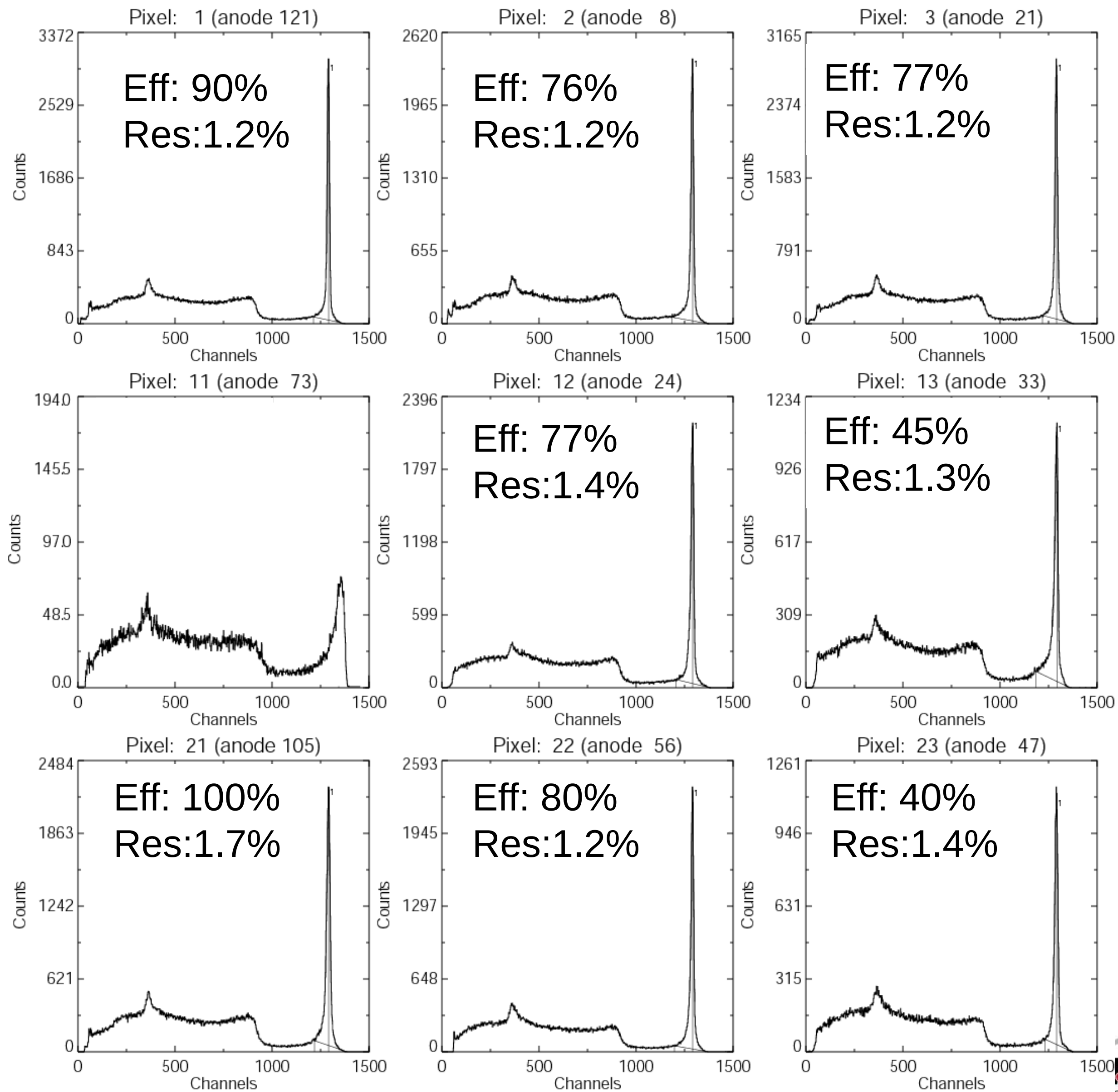

3x3 array: Rejecting ICC events in the case of ^{133}Ba source (low energy events) for three selected detectors

Original | Accepted | Rejected | Merit function

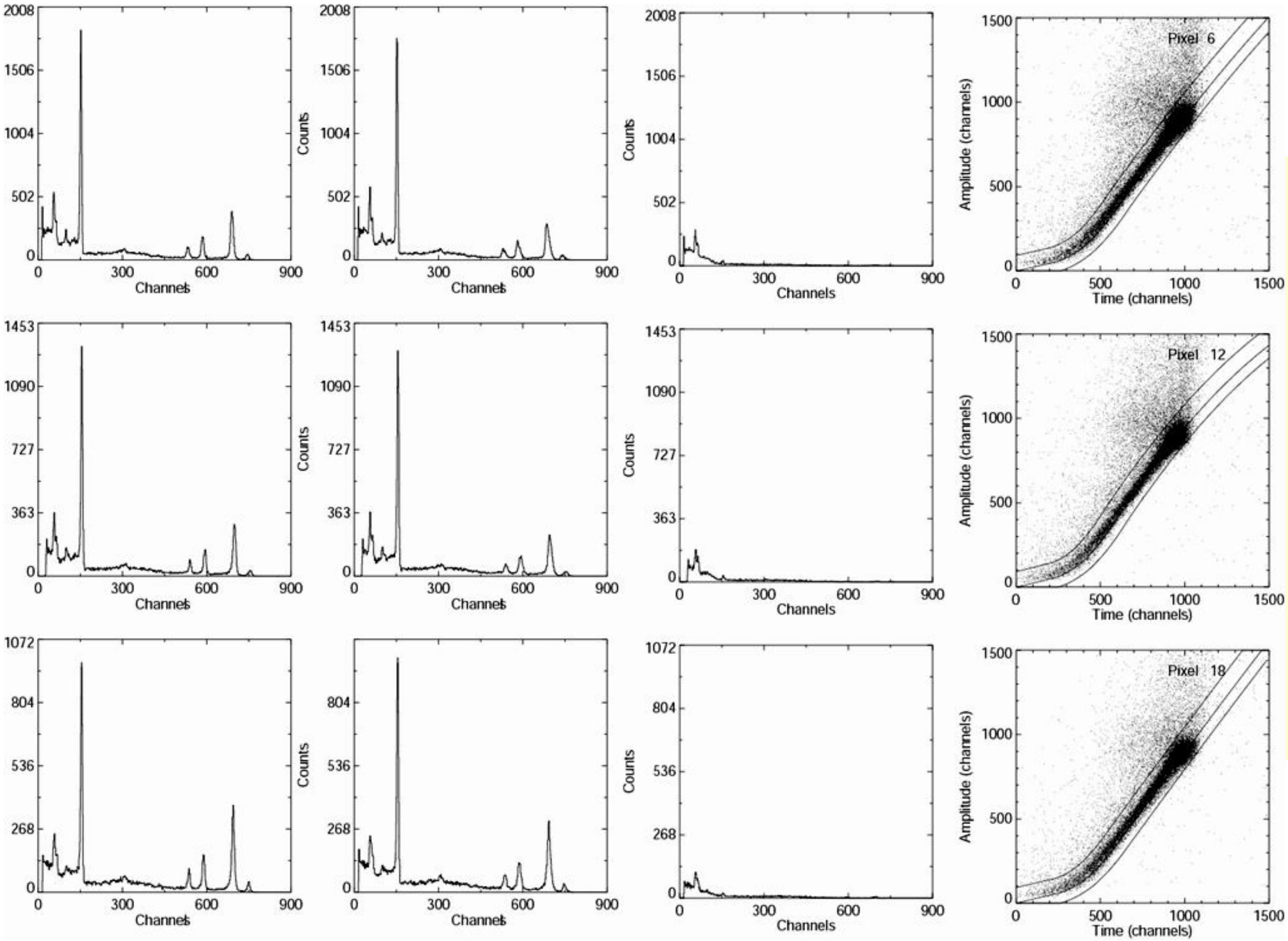

We use the same merit function obtained for high-energy gamma rays (662 keV)!

This mean that rejecting algorithm can be applied for the whole energy range

3x3 array: Spectra plotted for <u>two</u> interaction point events (^{137}Cs source)

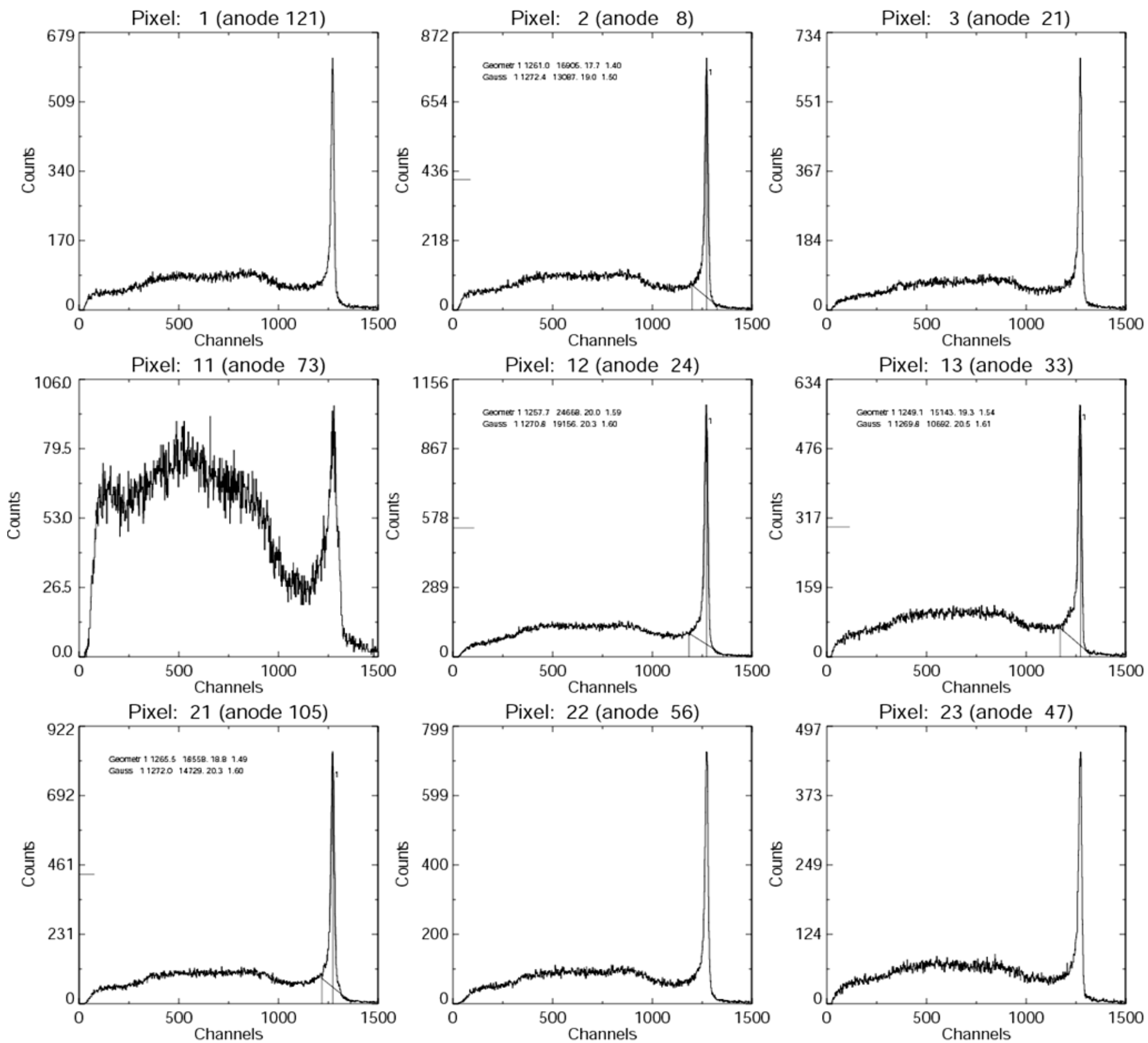

Signals from two detectors are added together

Energy resolution is in the range of 1.4-1.6% FWHM at 662 keV

3x3 array: Rejecting ICC events in the case of two interaction point events (^{137}Cs source)

Original spectra | Accepted | Rejected | Events distribution

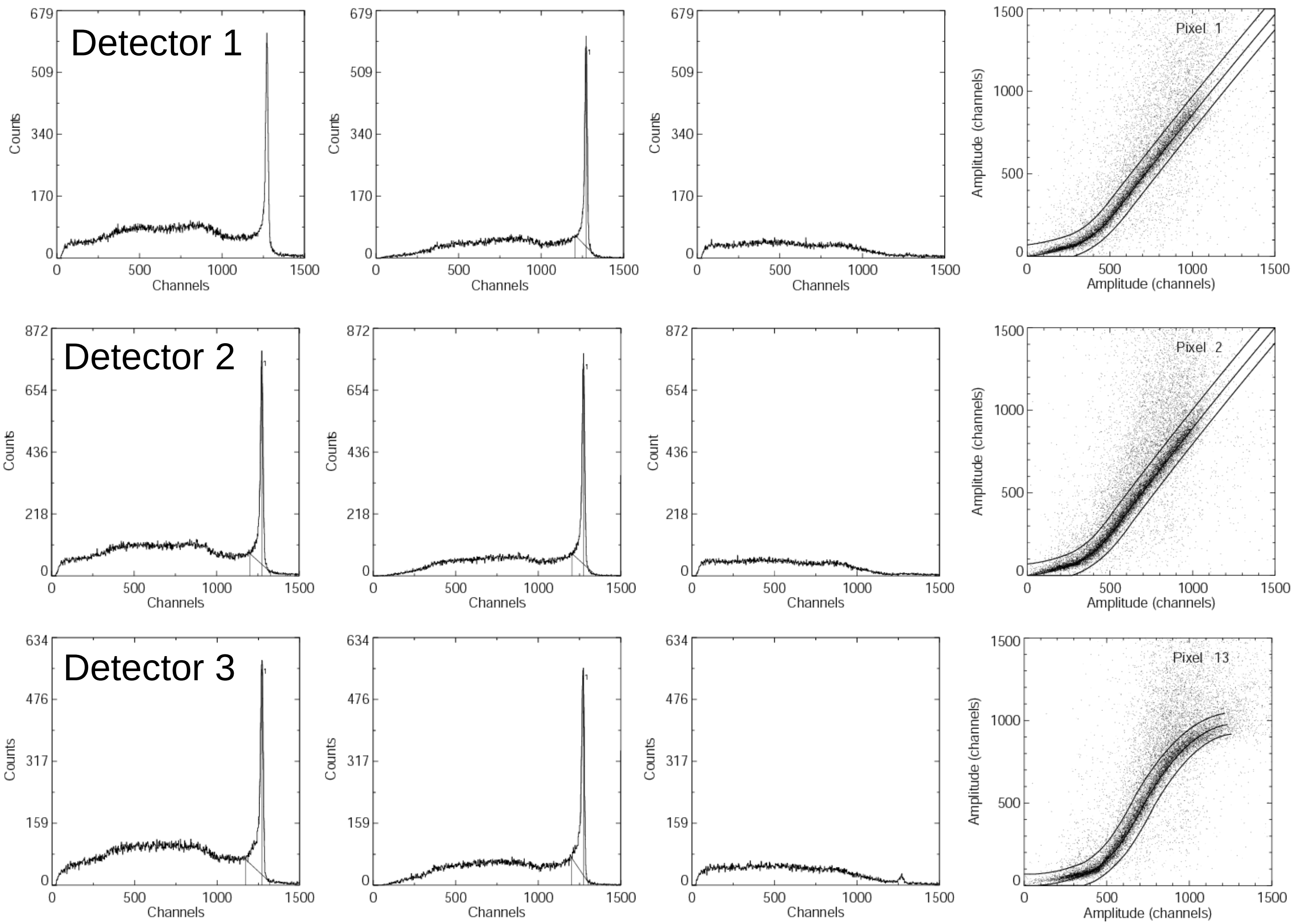

The merit functions were obtained from

$$C_i / A_i = \frac{C R_i(T_i)}{\sum A_j R_j(T_j)}$$

where, *Ri(Ti)* is a correlation function measured for single-point interaction events

Spectra for three interaction point events (^{137}Cs source)

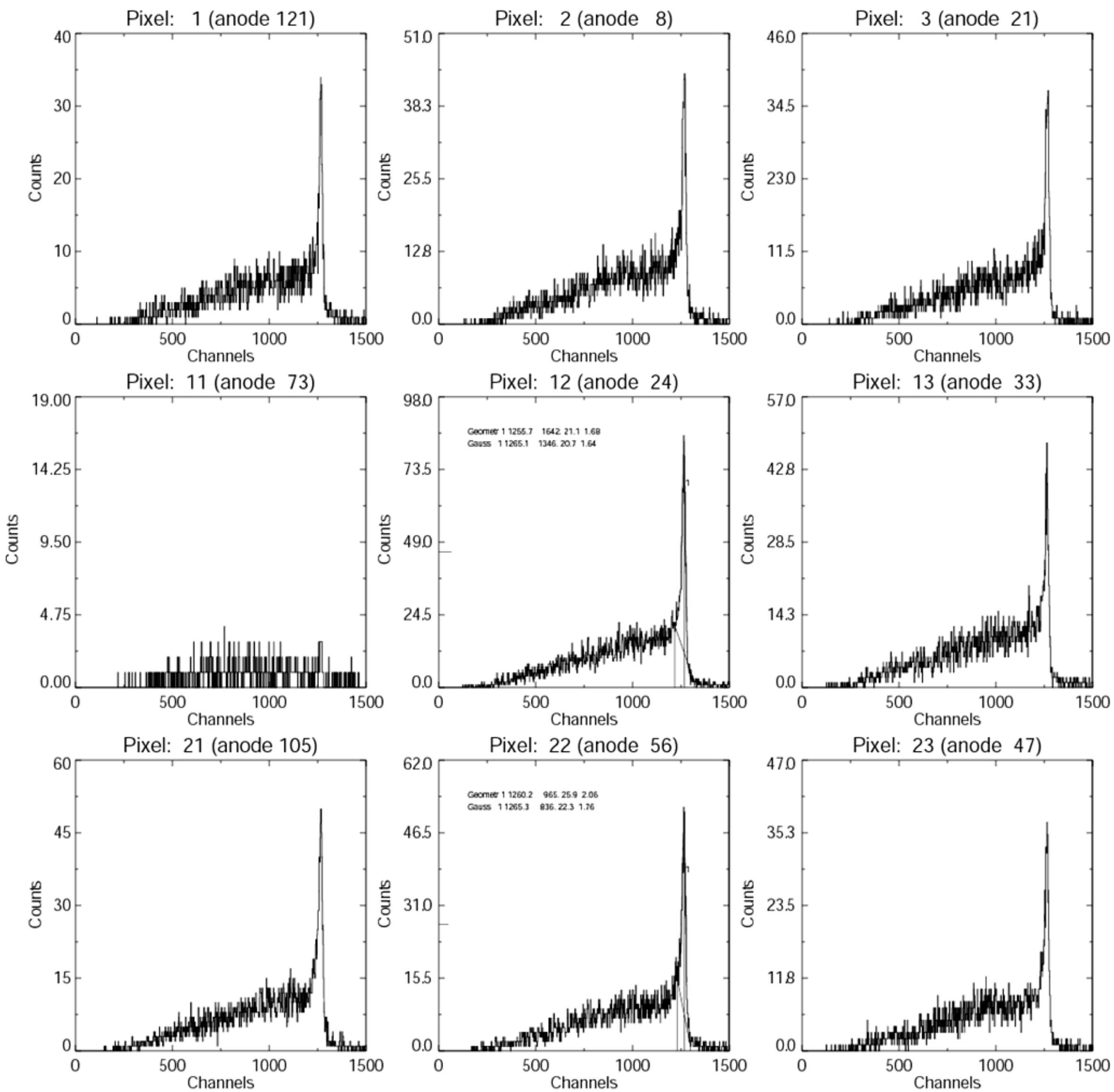

Signals from three detectors are added together

Energy resolution is in the range of 1.6-1.8% FWHM at 662 keV

3x3 array: Rejecting ICC events in the case of three interaction points events (^{137}Cs source)

Original spectra | Accepted | Rejected | Events distribution

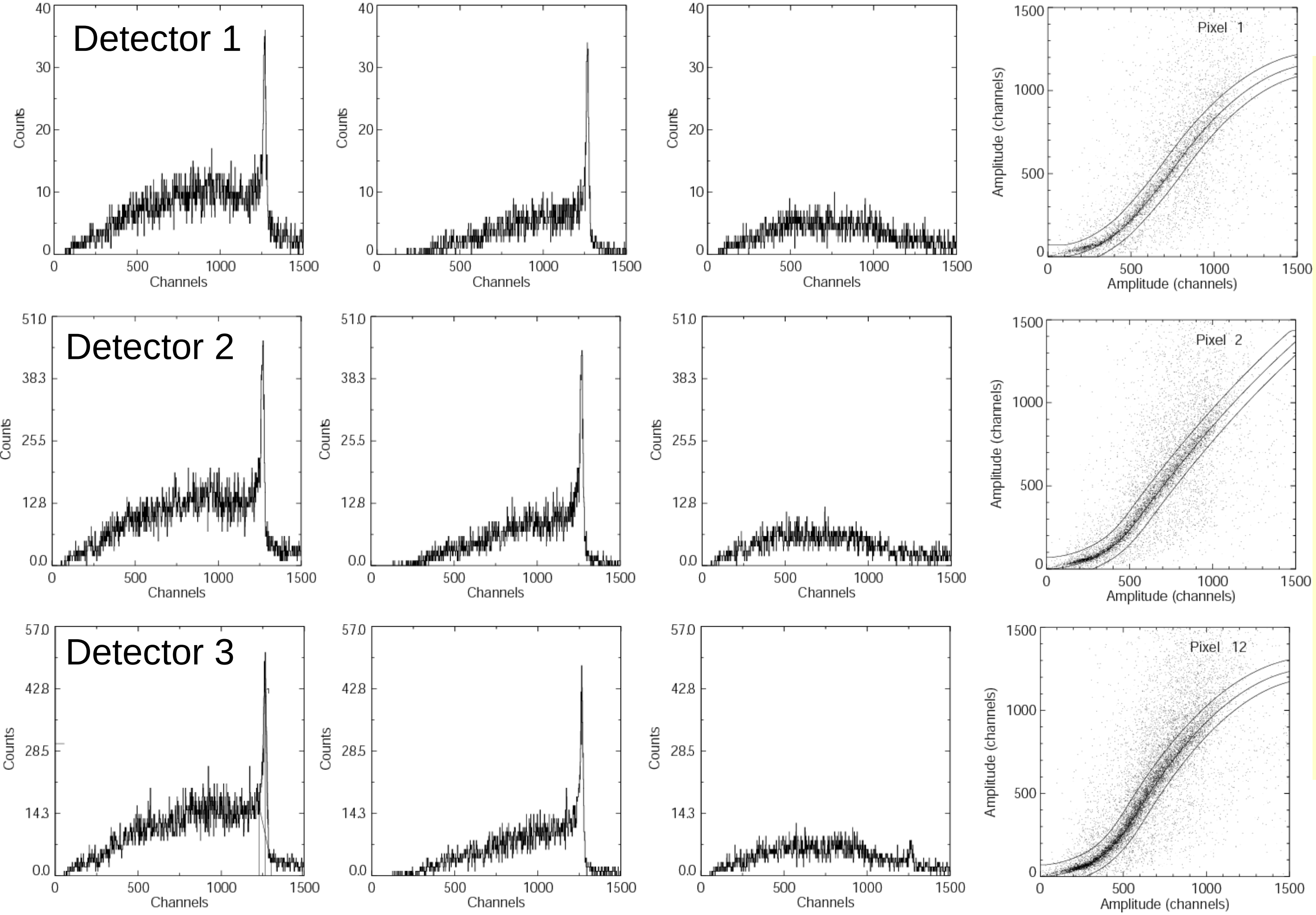

The merit functions were obtained by using the relationship

$$C_i / A_i = \frac{C R_i(T_i)}{\sum A_j R_j(T_j)}$$

where, *Ri(Ti)* is a correlation function measured for single-point interaction events

Conclusions

We validated designs and tested the performance of the virtual Frisch-grid detectors with a common cathode

We identify the requirements for the new ASIC, which is currently under development in BNL's Instrumentation Division

We validated the algorithm for rejecting the incomplete charge collection events caused by crystal defects in the cases of single and multiple interaction point events

Based on these results we are looking forward to integrating the first large area array

Acknowledgments

This work was supported by U.S. Department of Energy, Office of Nonproliferation and Verification Research & Development (NA-22) Office of Nonproliferation Research and Development, U.S. Defense Threat Reduction Agency (DTRA) and BNL's Technology Maturation Award.

Acknowledgements

Department of Nonproliferation and National Security: Giuseppe Camarda, Yonggang Cui, Anwar Hossain, Ge Yang, Dr. Ralph James Istvan Dioszegi, Leon Forman, Vinita Ghosh, Peter Vanier, Carl Czajkowski, Stephen Musolino, Joe Indusi, and Carol Kessler

BNL’s Instrumentation Division: Gianluigi De Geronimo, Emerson Vernon, Jack Fried, Graham Smith, Paul O'Connor, Peter Siddons, Paul Vaska, George Mahler, and Veljko Radeka